Applied Energy 228 (2018) 980–998

Contents lists available at ScienceDirect

Applied Energy

journal homepage: www.elsevier.com/locate/apenergy

Wind turbine selection method based on the statistical analysis of nominal specifications for estimating the cost of energy

Andrés Arias-Rosales*, Gilberto Osorio-Gómez

Design Engineering Research Group (GRID), Universidad EAFIT, P.O. Box 050022, Medellín, Colombia

HIGHLIGHTS

- Wind turbine selection method based on easily available nominal specifications.
- Cost of energy estimation when accessible information is limited or unreliable.
- Construction of a dataset with valuable information from 176 HAWT turbines.
- Statistical models of the efficiency and hub height were proposed and validated.
- Uncertainty assessment with prediction intervals and stochastic dominance analysis.

GRAPHICAL ABSTRACT

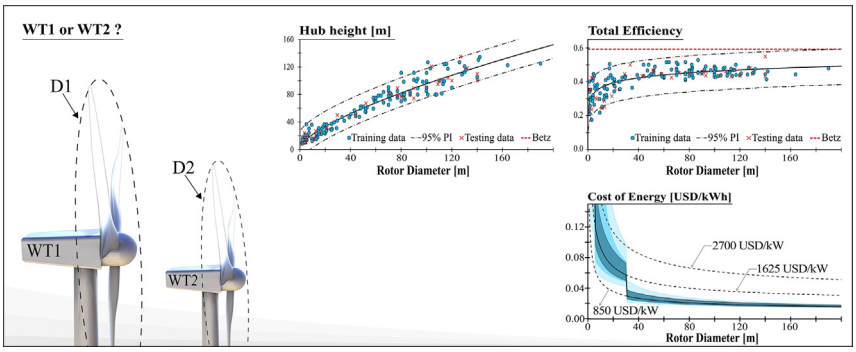

ARTICLE INFO

Keywords:
Wind turbines
Cost of energy
Statistical modeling
Selection method
Nominal specifications
HAWT dataset

ABSTRACT

Wind turbine selection is a critical engineering problem in the overall cost-effectiveness of a wind project. With the wide spreading and democratization of wind energy technologies, non-expert stakeholders are being faced with the challenge of selecting among very different wind turbines. As a comprehensive indicator, the cost of energy can serve as a guide, but reportedly misleading publicity and commonly unavailable information render its calculation more inaccessible and less reliable. Accordingly, this work proposes a method to compare wind turbines, on the basis of the cost of energy, from only nominal specifications and a standard characterization of the local wind conditions. For this endeavor, it was identified that two key variables are not usually available at a preliminary stage: the total efficiency and a feasible hub height. Through a systematic statistical analysis of the trends in a constructed dataset of 176 turbines, it was possible to establish regression models for the estimation of both variables. These models were tested in a validation set and their estimations were found to correctly characterize the central trend of the data without significant deviations. The uncertainty related to the use of both models was addressed by analyzing the 95% Prediction Intervals and the stochastic rank dominance. The established statistical models were then used as the core of the proposed selection method. When the available information is limited or not trustworthy, the steps of the method can be followed as an approach to estimate the cost of energy of a given horizontal axis wind turbine in a given location.

1. Introduction

Anthropogenic climate change [1], the growing urgency to reduce the world's dependence on fossil fuels, and a raising eco-friendly consciousness [2], are accelerating the democratization of renewable energies. Notably, the wind energy has experienced a steep growth rate

* Corresponding author.
E-mail addresses: aariasr@eafit.edu.co (A. Arias-Rosales), gosoriog@eafit.edu.co (G. Osorio-Gómez).

https://doi.org/10.1016/j.apenergy.2018.06.103
Received 8 March 2018; Received in revised form 26 May 2018; Accepted 21 June 2018
Available online 10 July 2018
0306-2619/

Nomenclature

Acronyms

CR	Certification Reports
HAWT	Horizontal Axis Wind Turbine
JM	Justus and Mikhail model for Weibull parameters extrapolation
LCOE	Levelized Cost Of Energy
ME1	Model of Efficiency where $\hat{\eta} = f_{(D)}$
ME2	Model of Efficiency where $\hat{\eta} = f_{(\eta_R)}$
ME3	Model of Efficiency where $\hat{\eta} = f_{(D,\eta_R)}$
MED	Model of Efficiency in function of Diameter
MHh	Model of Hub height where $\hat{Hh} = f_{(D)}$
MHhD	Model of Hub height in function of Diameter
MPr	Model of rated Power
PI	Prediction Intervals
RMSE	Root Mean Square Error
SR	Spera and Richards model for Weibull parameters extrapolation
SWT	Small Wind Turbine
TB	Trusted Brands
TP	Third-Party testing studies
WT	Wind Turbine

Greek symbols

$\overline{\eta}$	mean total efficiency
η	total efficiency
η_{95high}	estimate of the upper 95% PI limit in $\hat{\eta}$
η_{95low}	estimate of the lower 95% PI limit in $\hat{\eta}$
η_R	rated efficiency
λ	used in variable transformation, such as X^{λ}
ρ	air density in [kg/m^3]

Variables

$\overline{V}$	average wind speed in [m/s]
A	swept area in [m^2]
c	Weibull scale parameter
C_E	cost of energy in [USD/W h]
C_{wt}	wind turbine's cost in [USD]
D	rotor diameter in [m]
E	energy output in [W h]
E_0	energy [W h] under the increasing section of the Power Curve
E_R	energy [W h] in the nominal region of the Power Curve
$h1$	height [m] at which the Weibull parameters are measured
h_{asl}	height above sea level in [m]
Hh	hub height in [m]
Hh_{95high}	estimate of the upper 95% PI limit in $\hat{Hh}$
Hh_{95low}	estimate of the lower 95% PI limit in $\hat{Hh}$
I	real rate of interest
k	Weibull shape parameter
$Life$	lifespan in [years]
m	proportion of the operating and maintenance costs in terms of the capital cost for the whole project
nR	number of Riemann rectangles
P	power output in [W]
p	air pressure in [Pa]
P_R	rated power in [W]
r	Pearson's coefficient
R^2	coefficient of determination
T	air temperature in [K]
t	$Life$ given in [h]
V	wind speed in [m/s]
V_{Δ}	width of Riemann rectangles in [m/s]
V_{in}	cut-in speed in [m/s]
V_{out}	cut-out speed in [m/s]
V_R	rated wind speed in [m/s]
WT_p	proportion of the capital cost for the whole project represented by the turbines
X	predictor variable
Y	response variable
Z_0	surface roughness in [m]

since 1990 [3,4] in terms of implementation and research interest. This has contributed to the wind energy's transition to one of the most technologically mature renewable energies [5] and the fastest spreading energy source [6]. The main drivers of this trend are the three-bladed Horizontal Axis Wind Turbines (HAWTs). They are the most common Wind Turbines (WTs) and have more credibility in the market because of their balance regarding efficiency, cost-effectiveness, scalability, and social acceptance [7,8].

The overall cost-effectiveness of a wind project greatly depends on the WT selection in accordance with the wind conditions. As stated by Perkin et al. [9], "Poor turbine selection results in a financially sub-optimal investment". Correspondingly, a more efficient WT means that more usable energy can be extracted per cross-section area of the incident wind. This extra energy can help to outweigh the cost of investment. The overall efficiency, namely the *Total Efficiency* (η), is composed of: an aerodynamic efficiency for transforming the kinetic energy of the wind into mechanical energy in the axis of the rotor, a mechanical efficiency for transmitting this energy towards the axis of the electric generator, and an electric efficiency for ultimately generating electrical usable power.

Gipe [10] refers to a general well-known relation between the η of a WT and its size (in terms of rotor diameter and rated power), but he does not provide a full characterization of this relation. The electrical efficiency of HAWTs in the market is expected to be 96–97% for turbines rated at 2.5–3 MW (around 90–100 m in diameter), but only 60–70% for turbines rated at 0.5–10 kW (around 1–5 m in diameter) [11]. It has also been found that the bigger the rotor diameter, the bigger the Reynolds number related to the flow conditions [12,13]. Bak [14] found that a bigger Reynolds number allows a greater lift-to-drag ratio, which in turn tends to increase the aerodynamic efficiency. In agreement with these scaling implications, Bukala et al. [4] make a broad comparison from reported efficiency values: the η of modern big-scale HAWTs is around 45% while only 35% with Small Wind Turbines (SWTs).

Furthermore, Hren and Hren [15] state that, "As a general rule, wind energy becomes more cost-effective as wind turbines increase in diameter". The increment in usable energy, due to a bigger size, tends to be greater than the implications in the cost of investment and ecological footprint, which leads to more sustainable wind energy [16].

Accordingly, the global wind market is heading towards seemingly ever-bigger wind turbines, seeking a lower Levelized Cost Of Energy (LCOE) [17,18]. During 2012, the average capacity of new installed WTs was 4 MW per turbine (more than 110 m in diameter) [17]. WTs of up to 20 MW (around 250 m in diameter) may even be feasible in terms of LCOE with few technical improvements to face the extreme loads [18]. However, Ederer [17] warns that this trend must be critically challenged. After performing detailed LCOE analyzes for turbines with different rated power specifications, he stated that, in terms of market

equilibrium, it is not reasonable to develop WTs beyond 10 MW (around 175 m in diameter). Hence, it is crucial to assess the impact of size on the cost of energy when comparing and selecting turbines.

The size of the rotor is related to the *Hub height* (*Hh*), which can be decisive in energy calculations [19,20]. As the rotor moves higher above the ground, stronger winds (on average) are available because the friction with the terrain decreases. This relation between mean wind speeds and height is usually modeled with the well-known wind profile Power [21] and Logarithmic [22] laws. Extrapolations drawn from these models are considered rough yet valid and useful estimations within the lower atmospheric layer, i.e., around 150–200 m above ground level [23]. The parameters of Weibull probability distributions, commonly used to characterize the wind conditions of a given location, can also be extrapolated in function of *Hh* with several methods [24,25].

As seen in the wind energy market, bigger rotors tend to make higher towers feasible. This allows the rotor to be exposed to better wind conditions with more energy to be harvested [26]. Nevertheless, beyond the lower atmospheric boundary layer, the wind profile does not necessarily imply stronger winds, so the incentive to increase *Hh* goes only up to a point. Also, taller WT towers imply an additional cost of investment [9]. Accordingly, the assessment of *Hh* in relation to the *Rotor Diameter* (*D*) is key to the problem of comparing and selecting WTs.

Numerous methods were found in the literature which support the WT comparison and selection through energy and cost assessments. Ederer [17], Perkin et al. [9], Montoya et al. [27], Alam et al. [19], and Drew et al. [28] performed such analyzes with energy estimations based on Power Curves, which characterize the expected power that a given WT can deliver in function of the wind speed. But Power Curves, in addition to other detailed information commonly used to estimate the energy output, are not always easily accessible or reliable [9,15]. An investor or buyer who is offered several WTs often must rely on the rated power specification, which is reportedly a poor direct estimator of the actual yield [10]. There have been reported cases of unrealistic energy expectations based on misleading marketing strategies, as well as unreliable Power Curves [4,10]. This issue is more severe with SWTs [29] due to a market that is less regulated, relies more on marketing strategies than in feasibility studies, and is usually influenced by decision-makers and stakeholders who are non-experts in wind energy.

Some works have faced the unsuitability or unavailability of Power Curves by constructing them through data-driven methods. For instance, Üstüntaş and Şahin [30] used cluster center fuzzy logic to model the Power Curves of specific WTs. However, this method requires previously measured power data from each turbine at the same location where it is to be implemented. Similarly, Li et al. [31] performed power estimations through artificial neural networks and regression models that were fitted to existing wind speed, wind direction, and power measurements. With the same modeling purpose and with similar data availability imitations, Janssens et al. [32] tested a series of machine learning algorithms, such as k-nearest neighbors and Random forest. Díaz et al. [33] also approached power estimation with machine learning but they departed from available Power Curves and used data-driven algorithms to estimate the wind speed and air density conditions.

Other reviewed approaches require less detailed information for power or energy estimations. Some studies simply assume constant generic η values for HAWTs [4,34,35]. Once the efficiency η and the Weibull parameters are known, standard equations can be used to estimate the power and then the energy [10]. Other researchers used generic up-scaling laws for mechanical equipment to estimate the effect of WT size on costs, ecological footprint and power [16,18]. On the other hand, some methods estimated the Power Curve of a given set of WTs from equations based on the rated power, the rated speed, the cut-in speed, and the cut-out speed [36,37].

D and *Hh* have been reported as key predictors in the assessment of WT cost-effectiveness [16,17]. As Gipe [10] states, “The most reliable indicator of how much electricity a wind turbine will generate is its rotor diameter”. However, the reviewed methods that can be used for comparing WTs do not establish a clear general relation between *D*, η, and *Hh*. Consequently, seeking to enable a well-informed energy and cost calculation, this work establishes and validates general statistical relations between *D*, η, and *Hh*. The resulting models are then used as the core in the proposal of a method for comparing and selecting HAWTs on the basis of the cost of energy. To the best of the authors’ knowledge, the following are the contributions of this work to the state of the art:

- The construction of a dataset with the nominal specifications and efficiency values of 176 commercialized HAWTs. Available at [38]. (Section 3)
- Establishment of a statistical relation between the rated power and the diameter, which was compared with previously reported relations. (Section 3)
- Systematic statistical analysis of the total efficiency and the hub height in relation to nominal specifications. This resulted, respectively, in the proposal and validation of the models MED (Model of Efficiency in function of Diameter) and MHhD (Model of Hub height in function of Diameter). (Sections 4 and 5)
- Analysis of the uncertainty related to the proposed models, including a new approach to assess the stochastic rank dominance. (Sections 4.3 and 5.3)
- Wind turbine selection method based mainly on easily available nominal specifications. (Section 6)
- The steps of the method also serve as an approach for estimating the cost of energy of a given HAWT and location when the information is limited, incomplete, or unreliable. (Section 6)

2. Description of the applied problem

This section describes the applied engineering problem of selecting among different commercial HAWTs, on the basis of cost-effectiveness, with only nominal specifications and a standard characterization of the local wind conditions at hand. With the increasing democratization of wind technology and a growing diversification of commercial options, more and more non-experts are being challenged with the WT selection problem. In this work, non-experts refer to professional engineers, designers, architects or general stakeholders who are directing the decision-making process for the selection of a wind turbine, but who do not have a specialized academic or professional background on the implementation of wind energy. This is the case, for instance, of an architect looking at online offers of SWTs for a “green building”. Another example can be a community of neighbors getting together to buy and install a relatively big WT to meet part of their energy demand in a rural location, a strategy that is already common in Denmark, Germany and France [10].

Unfortunately, this accelerated democratization of the technology has given room to less regulated commercial offers. This scenario is triggering controversial unsustainable implementations, caused partly by fierce commercial competition and misleading advertising. As described in Section 1, the most common controversial implementations are related to small wind turbines. However, poor WT selection, due to misleading advertising, has also affected projects on a bigger scale, such as with the more than 500 Darrieus WTs installed in California in the 1980s. These WTs were developed by FloWind and were promoted with highly inflated power ratings, which led to over-prized wind farms [10]. Hence, the wind turbine selection is a critical applied problem that greatly affects the overall cost-effectiveness of a wind project.

One approach to assess and compare WTs in terms of cost-effectiveness is to calculate the cost of energy [USD/kWh] by considering the total costs and the energy expected to be produced throughout the entire lifespan. The total cost can be directly estimated from the

commercial prize of the WTs offered and with common financial assumptions [39,40]. However, how can we estimate the total expected energy production? In the first place, the wind conditions must be determined for the given location where the WTs are planned to be installed. The Weibull probability distribution function is usually used for modeling the wind speed conditions by adjusting its Shape (k) and Scale (c) parameters to fit measured data [41]. Wind speed data is usually measured at a standard 10 m above ground level [22], so the Weibull parameters must be extrapolated to the *Hub height* (*Hh*) [42].

In principle, one could arbitrarily define *Hh* for a given WT. Nevertheless, the definition of *Hh* implies a cost-benefit situation: higher towers tend to expose the rotor to stronger winds, but higher towers also tend to increase the capital costs. The optimal *Hh* for a given *WT* will ultimately depend on a series of specificities in terms of cost and the wind patterns of a given location. When such specificities are not accessible to a non-expert comparing WTs, and the commercially provided information about tower heights is ambiguous, there is a need for a model that allows a tentative *Hh* estimation.

Once the wind conditions are known at *Hh*, it is necessary to establish how the *Power Output* (P) [W] varies in function of the *Wind Speed* (V) [m/s]. This is what Power Curves are used for. However, Power Curves are not always easily accessible or reliable when acquired from an unregulated distributor (see Section 1). For instance, Fig. 1 presents two considerably different Power Curves describing the performance of the same WT, i.e., the XZERES ARE 442 from Abundant Renewable Energy (ARE). One curve was commercially available (by ARE) while the other was obtained from a third-party study of NREL [43]. Such discrepancies may be caused by too idealistic conditions assumed by promoters. This figure also presents the rated conditions, namely the *Rated Power* (P_R) and the *Rated Wind Speed* (V_R). P_R is supposed to be met at 11 m/s but this power is never achieved along the NREL Power Curve.

When trustworthy Power Curves are not available, they can be constructed with the well-known [10,41] Eq. (1).

$$P = \frac{1}{2}\rho A \eta V^3 \tag{1}$$

With ρ = Air Density [kg/m^3], A = Swept Area [m^2], and η = Total Efficiency. An average ρ can be estimated for the location of interest or a standard 1.225 kg/m^3 (at sea level) may be used. A can be directly calculated from D. Also, the behavior of V is defined by a Weibull distribution with its parameters extrapolated at *Hh*.

However, how can we obtain η when only nominal specifications are available? One possible approach is to use the *Rated Efficiency* (η_R) instead of η. η_R can be calculated by solving Eq. (1) for η but with P_R instead of P and V_R instead of V. The case of a Power Curve constructed from η_R is illustrated in Fig. 2 for the wind turbine CF20 from C&F Green Energy. For this WT, η_R = 33.23%. This curve is compared here with a trustworthy Power Curve obtained from an Intertek Testing Services [44] certification report for the same WT. There is an evident mismatch between these curves that could lead to over-optimistic energy calculations if η_R were to be used directly. For instance, according to the V_R specified for the CF20, P_R = 20 kW should be achieved at 9 m/s. However, P_R is achieved at 10.5 m/s according to the Intertek's study. Similar to P_R, η_R is, by itself, a misleading performance estimator and this is evidenced in the divergent η_R-constructed curve.

On the other hand, if η could be estimated from statistical trends extracted from commercial HAWTs, better Power Curves may be obtained. This is one of the main hypotheses that this work seeks to explore. To analyze whether such η trends exist and are in fact useful, a dataset must be constructed. This dataset should contain the η values of a representative number of HAWTs and their nominal specifications so that potential statistical relations between them can be modeled. The η values can be calculated if trustworthy Power Curves are available for the WTs of the dataset, such as with the example presented in Fig. 2. Here, from the Intertek's Power Curve, a series of horizontally equidistant points are taken, resulting in (V, P) 2-tuples. η can be obtained at every point with Eq. (1). The maximum η is then established as the representative total efficiency for the corresponding WT. Even though η can vary in function of V, Bukala et al. [4] found that it can be assumed as constant without a considerable error in energy calculations. Establishing a constant η is a common practice for comparison matters [4,34].

In the case of this example (Fig. 2), the resulting η was 25.16%. The figure shows how the Power Curve constructed with this efficiency closely resembles the original Intertek Power Curve. It is worth noting that Power Curves usually get stabilized at P_R. This behavior reflects the real performance of most commercial WTs, which are aerodynamically or mechanically limited at this point seeking a smoother and more predictable power production. This transition is progressive, as can be seen in the Intertek curve of the CF20. Conversely, the P_R limitation is modeled with a common conditional truncation in the constructed Power Curves. It can also be noted that the curve obtained from Intertek starts increasing from around 3.5 m/s. This is in accordance with the specified *Cut-in Speed* (V_{in}) of 2.2 m/s, as no power is expected to be generated below this limit.

Through the analysis described in this section, it can be stated that a common applied problem in wind energy is when non-experts must select among commercial wind turbines with only nominal specifications at hand. If this selection process is based on cost-effectiveness, several variables are needed which are not always easily accessible, such as the hub height and the total efficiency. Therefore, this work aims at exploring statistical models for estimating such variables and use these models as the basis to propose a wind turbine selection method.

3. Development of the dataset

By examining the sources described in this section, a dataset of 176 commercial HAWTs was developed. The dataset is publicly available at [38]. The main purpose of this dataset is to explore and validate possible general statistical models for estimating η and *Hh*. It is worth noting that the turbines contained in this dataset are only a subset of the total population of commercialized HAWTs. Thus, the parameters of the statistical models that are proposed and tested in this work might be influenced by the possible biases in the dataset. Accordingly, this section provides a general description of the data, which can be used to assess whether the models proposed in this work apply to other specific cases.

For every turbine, the dataset includes the corresponding values of D, η, and η_R. The value of *Hh* was also gathered whenever possible. The turbines were randomly assigned to two groups: a Training set with 80% of the data, which is used for exploring and establishing statistical trends, and a Testing set with 20% of the data, which is used for validating the models proposed. Thus, for modeling η, there were 140 WTs for training and 36 for testing. As the information related to *Hh* (e.g., commercialized towers) was not always available, the set for exploring trends related to *Hh* is composed of 126 WTs for training and 32 for

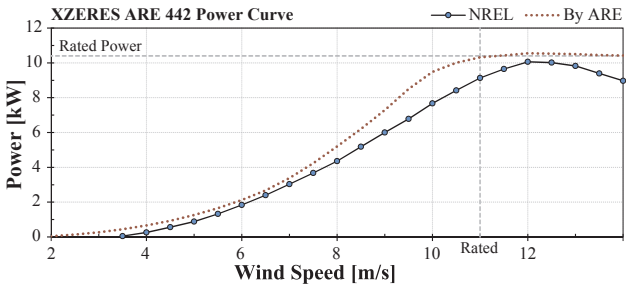

Fig. 1. Power Curve of the XZERES ARE 442 from Abundant Renewable Energy (ARE), with a 7.2 m diameter.

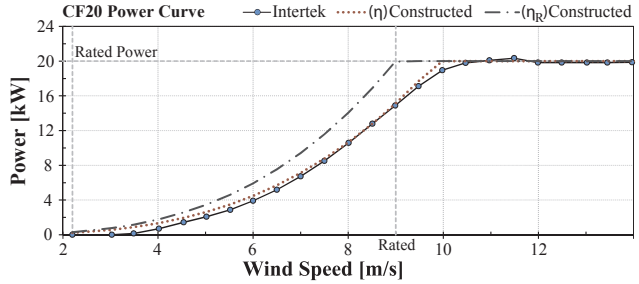

Fig. 2. Power Curve of the CF20 from C&G Green Energy, with a 13.1 m diameter.

testing.

The procedure followed for estimating the η of every turbine in the dataset was described in Section 2 and the result of this procedure is illustrated in Fig. 2. In the same figure, it was evidenced that η_R is, by itself, a misleading performance estimator. However, η_R might be of use as a possible predictor for statistical η and Hh models, which is explored in Sections 4 and 5. Accordingly, η_R was calculated for every turbine with the procedure explained in Section 2. In terms of *Hh*, this work hypothesizes that there is a range of hub heights, for a given *D*, that tends to be more feasible in terms of cost-effectiveness, regardless of the specificities. To explore this hypothesis, this work assumes that, if such a trend exists, it might be evidenced statistically in the WT towers offered commercially. Thus, when the information was available, *Hh* was calculated as the average between the heights of the different towers offered commercially for every WT.

As stated in Section 1, the misleading marketing strategies and controversy are mostly associated with SWTs [10,29]. Therefore, with respect to SWTs, this work assumes as trustworthy the information related to Power Curves when it is originated from Certification Reports (CR) or Third-Party testing studies (TP), as suggested by the literature [10,45]. The rest of the turbines were taken from publicly available information delivered by Wind Turbine brands assumed to be trustworthy. The WTs from these Trusted Brands (TB) range from a minimum $D = 13$ m (FuhrLänder FL 30) to a maximum $D = 190$ m (amsc Seatitan 10 MW) and with a mean $D = 78.5$ m. Table 1 presents the No. WTs grouped by source.

Fig. 3 presents how the WTs from the different sources are distributed in terms of 3(a) *D* and 3(b) P_R. To improve comparisons, the groups are sorted by their median values and the rated power is shown in logarithmic scale (Y-axis in 3(b)). It is illustrated how the certification reports and third-party studies were focused around smaller diameters, mostly below 20 m, as opposed to the Trusted sources.

On the other hand, Fig. 4 presents how the WTs from the different brands are distributed (sorted by the median) in terms of 4(a) *D* and 4(b) P_R. From Figs. 3 and 4, a relation between P_R and *D* can be evidenced, which is explored further in Fig. 5. Engels et al. [59] established regression models by fitting the function $Y = \alpha X^{\beta}$ to existing data, where $Y = P_R$ and $X = D$. They presented three regression models corresponding to different wind classes. Fig. 5 shows the trend-lines of these models (named as Class I Prediction, Class II Prediction, and Class III Prediction) estimated for the dataset of this work. Their Root Mean Square Error (RMSE) resulted in 908.6 kW, 569.3 kW, and 548.9 kW, respectively.

The same regression model $Y = \alpha X^{\beta}$ was fitted to the dataset in Python 2.7 using the *Curve_fit* algorithm from the *Scipy.optimize* package [60]. This resulted in the MPr (Model of rated Power) described by Eq. (2), with P_R in [W]. The RMSE for MPr was 547.7 kW. As shown in Fig. 5, the trend-line estimated with MPr is visually in good agreement with Class II Prediction and Class III Prediction.

$$MPr = \widehat{P_R} = 342.6D^{1.928} \quad (2)$$

Even though P_R is widely used as a first means for comparing commercial WTs, Gipe [10] warns that there is an "unreliable and often misleading shorthand" for energy estimations. Nonetheless, MPr can be used to assess whether the P_R of a given turbine is in accordance with the commercial trends found in the dataset constructed in this work. For instance, a P_R value that is considerably higher than what can be estimated with Eq. (2) may suggest that P_R is less trustworthy as a performance indicator in that particular case.

4. Statistical modeling of the Total Efficiency

The purpose of this section is to explore whether a valid statistical model for estimating the *Total Efficiency* (η) can be established in function of variables obtained from the nominal specifications. The predictor (independent) variables examined are *D* and η_R for reasons discussed in Sections 1 and 2. A range of linearization transformations are applied to the predictor variables. Then, a series of Simple and Multiple Linear Regression models are fitted to the Training set with the transformed predictors. Among these possible models configurations (i.e., their explored hyperparameters [61]), three Efficiency models candidates are selected based on a 5-fold cross-validation analysis. These candidates are fitted to the whole Training set and then statistically evaluated in the Testing set. The model with the best estimation performance is established as MED (Model of Efficiency in function of Diameter). Finally, MED is further explored in terms of the uncertainty involved in estimating $\hat{\eta}$ for WTs outside the Training set.

Most analyzes in this section were programmed using Python 2.7. The *Pandas* package was used for dealing with data structures, *Sklearn.linear_model* was used for regression modeling, *Scipy.stats* for evaluating the linear correlation and normality, and *Random.choice* for programming the Monte Carlo procedures used. The Bootstrapping procedures used for the Prediction Intervals were programmed in R 3.4.3 with the *Mosaic* [62] package.

Table 1
No. WTs in the dataset grouped by source.

	Sources	No.
CR	Intertek Testing Services NA, Inc. [44]	16
	Small Wind Certification Council (SWCC) [46]	12
	SGS Tecnos [47]	1
	GL Garrad Hassan's WINDTEST [48]	1
	Danish Technical University (DTU) [49]	1
TP	NREL [43,50–52]	5
	Wulf Test Field study [53]	4
	Warwick Wind Trials Project [54]	4
	Western North Carolina study [55]	4
	Zeeland report [56]	3
	USDA-Agricultural Research Service [57]	1
	STEP [58]	1
TB	Vestas Wind Systems	20
	ENERCON GmbH	20
	Fuhrländer AG	11
	Gamesa	10
	Nordex	10
	Siemens Wind Power GmbH	9
	GoldWind	8
	AMSC's Windtec Solutions	7
	General Electric Renewable Energy	7
	Northern Power Systems	5
	NEG Micon	5
	LagerWey	3
	Other	8

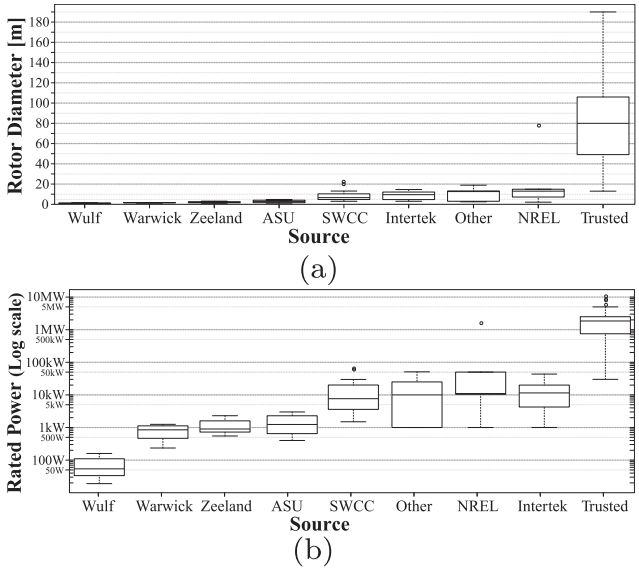

Fig. 3. Box Plots of (a) the Rotor Diameter and (b) the Rated Power in function of the information source.

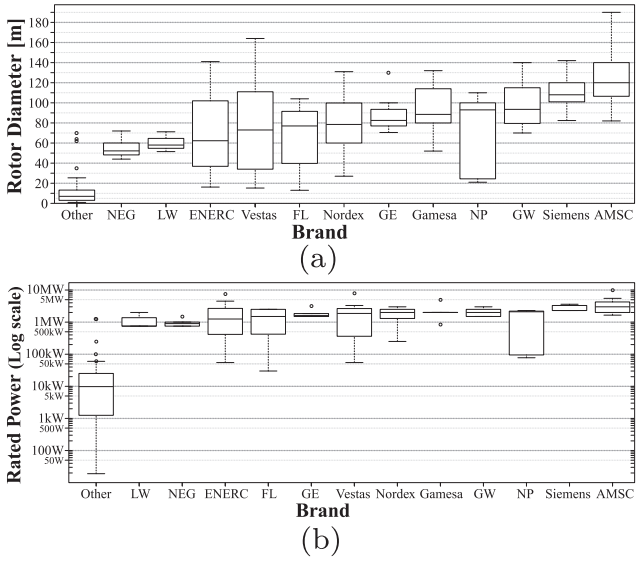

Fig. 4. Box Plots of (a) the Rotor Diameter and (b) the Rated Power in function of the Wind Turbine Brand.

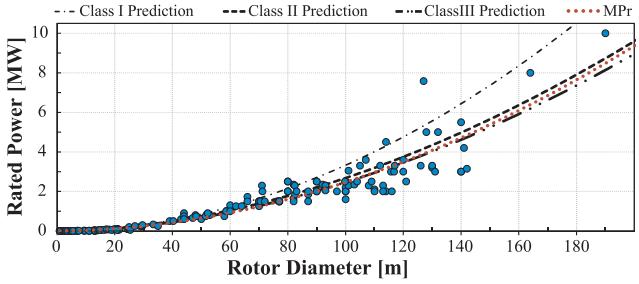

Fig. 5. Rated Power in function of Rotor Diameter.

4.1. Efficiency models candidates: modeling

In this subsection, potential statistical models of η (*Response variable Y*) are systematically explored in function of D and or n_R (*Predictors X*). It must be noticed that the regression models of this exploration do not assume direct causality regarding η. It is well known that the total efficiency of a given wind turbine depends on a plurality of technical specificities. On the contrary, these models intend to analyze whether simple and easily-available nominal variables can be of any use in the estimation of $\hat{\eta}$ by means of broad trends as opposed to precise values. For this exploration, linear regression models are used because of their simplicity, the clarity of interpretation and the inferential tools available for such models. Linear models are widely used in physical applications and are part of the core of statistic analyzes [63]. However, if statistical trends are in fact present in the data, they are not necessarily linear in nature. Accordingly, Tukey [64] proposed the "Ladder of powers". This simple procedure can be used to explore whether the data can be satisfactorily linearized by transforming the variables in the form X^{λ} and or Y^{λ}. However, only the predictors X are transformed in this work to avoid possible re-transformation biases [65]. λ is usually iterated through a range from -3 to 3 in steps of 0.5, and *Ln* (natural logarithm) is used when $\lambda = 0$ [64]. Seeking to improve the linearization resolution, λ is iterated here in steps of 0.01.

To evaluate the hyperparameters involved, i.e., λ and the variable or variables selected as predictors X, a 5-fold cross-validation analysis [32] was performed for every combination that was considered. 5 folds were used to preserve the 80% proportion of every cross-validation training set within the whole Training set, which is the same proportion of the whole Training set within the complete dataset.

The following analyzes were performed:

- ME1: $\hat{\eta} = f_{(D)}$. The Total Efficiency is estimated as a function of the rotor Diameter.
- ME2: $\hat{\eta} = f_{(\eta_R)}$. The Total Efficiency is estimated as a function of the Rated Efficiency.
- ME3: $\hat{\eta} = f_{(D,\,\eta_R)}$. The Total Efficiency is estimated as a function of the rotor Diameter and the Rated Efficiency.

Fig. 6 presents the original predictor and response variables without transformations ($\lambda = 1$). The relation is more evident in Fig. 6(a), where the data presents a smooth "bulge" [66] that may be effectively linearized by Tukey's procedure.

The results from iterating λ, according to Tukey's Ladder of powers, are presented for D^{λ}, in Fig. 7(a), and for n_R^{λ}, in Fig. 7(b). Every λ value was evaluated 5 times during the 5-fold cross-validation procedure and the performance was measured with the mean *Coefficient of Determination* ($\overline{R^2}$), the mean *Pearson's Coefficient* ($\bar{r}$), and the mean *Root Mean*

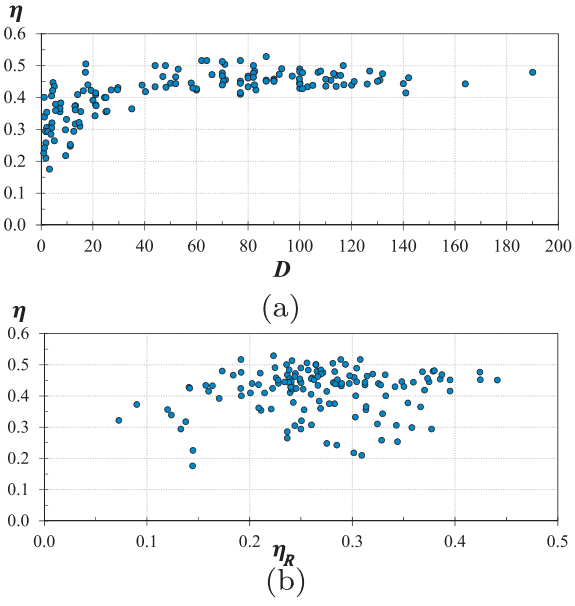

Fig. 6. Response variable η plotted against predictors D, in (a), and η_R, in (b).

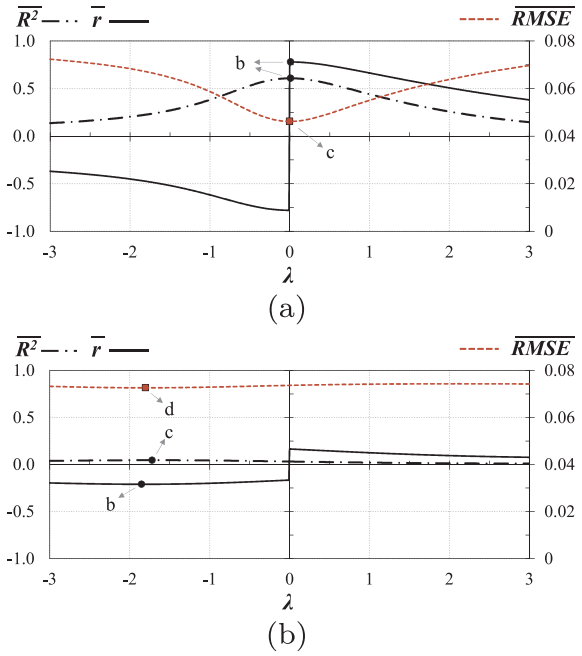

Fig. 7. Cross-validation evaluation of Tukey's Ladder of powers, iterating λ for D^{λ}, in (a), and n_R^{λ}, in (b).

Square Error ($\overline{RMSE}$). For every fold, R^2 and r were calculated with the cross-validation training set, while RMSE was calculated with the cross-validation testing set.

r measures the linear correlation between the predictor X and response Y variables [67]. R^2 measures the "share of Y variance explained by X variance" [68]. The larger R^2 is, the more useful a defined X variable is for estimating Y. Moreover, the smaller RMSE is, the more accurate the estimates on average. Based on this, the points where every performance curve was optimized (within the limitations of this work) were highlighted in Fig. 7 as points of interest.

Table 2 presents the results for the points of interest in the analyzes ME1 and ME2. For ME3, The 12 combinations of the hyperparameters of interest from ME1 [a-c] and ME2 [a-d] were tested with Multiple Linear Regressions. Row "a" shows the results for the untransformed predictor variables, which can be used as a comparison reference and to understand the impact of the linearization procedure. In the three ME analyzes the performance indicators were improved by means of the linearization procedure.

ME1b, ME1c, and ME3b were selected as the Efficiency models candidates. These three combinations of hyperparameters presented the best behavior in terms of maximizing $\overline{r}$ and $\overline{R^2}$, and minimizing $\overline{RMSE}$. The three models were fitted to the whole Training set (see Fig. 8). In this way, the corresponding parameters (i.e., the slopes and intercepts) were obtained with all the information available except for the Testing set so as not to influence the validation. The parameters of the resulting

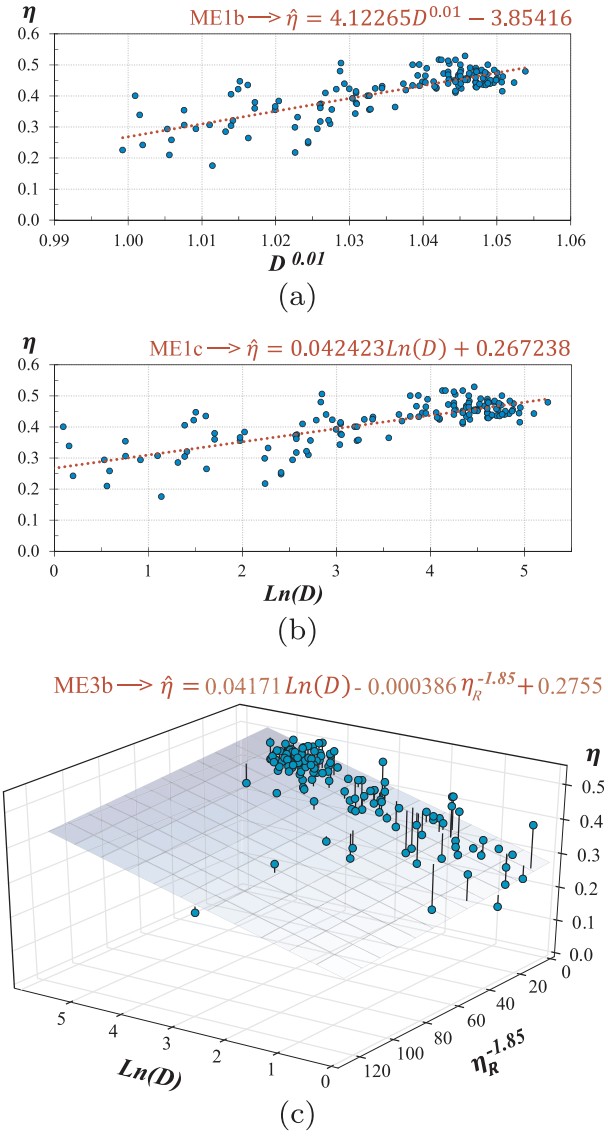

Fig. 8. Efficiency models candidates fitted to the whole Training set: ME1b in (a), ME1c in (b), and ME3b in (c).

regression models are shown in Fig. 8. From Table 2 and Fig. 8(a)-(b), it is evident that the fitting performance of ME1b and ME1c is almost identical. Moreover, these figures, in comparison with Fig. 6(a), illustrate that the linearization procedure was effective. Therefore, no further non-linear regression analyzes will be performed.

On the other hand, Fig. 8(c) reveals that the data in ME3b is mostly organized in response to $Ln(D)$ while the plane is pulled by a few points in the $\eta_R^{-1.8}$ direction. It is worth noting that ME1b and ME1c achieved a

Table 2
Points of interest in the cross-validation evaluation of Tukey's Ladder of powers, iterating λ for D^{λ} and n_R^{λ}.

	ME1				ME2				ME3			
	X	$\overline{r}$	$\overline{R^2}$	$\overline{RMSE}$	X	$\overline{r}$	$\overline{R^2}$	$\overline{RMSE}$	X	$\overline{r}$	$\overline{R^2}$	$\overline{RMSE}$
a	D	0.66357	0.440669	0.05510	η_R	0.1254	0.02049	0.074172	D, η_R	0.6636, 0.1254	0.4423	0.05571
b	$D^{0.01}$	0.77961	0.608094	0.04618	$\eta_R^{-1.85}$	-0.2098	0.04591	0.072627	$Ln\,(D)$, $\eta_R^{-1.85}$	0.7796, -0.2098	0.6139	0.04601
c	$Ln\,(D)$	0.77960	0.608086	0.04617	$\eta_R^{-1.72}$	-0.2096	0.04600	0.072630	-	-	-	-
d	-	-	-	-	$\eta_R^{-1.8}$	-0.2098	0.04597	0.072626	-	-	-	-

The results with the best performance are underlined.

fitting performance very similar to ME3b despite having only D^{λ} as the predictor variable. This is in agreement with the results in Table 2, where η_R^{λ} as the single predictor (ME2) presented a clearly worse fit compared to D^{λ} as the single predictor (ME1).

The residuals from the fitted regression models (Fig. 8) were tested for normality. With Shapiro-Wilk tests, it was revealed that these residuals were not normally distributed: P-value = 0.0037 for ME1b, P-value = 0.0033 for ME1c, and P-value = 0.0022 for ME3b. However, these deviations from the ideal behavior of regression residuals were expected because it is known that η is probably in function of more variables than the ones established in these models as *Predictors*. This is one limitation of this work considering that only nominal specifications are sought as inputs for the statistical models.

As normality cannot be assumed, parametric statistical analyzes should not be used. Therefore, Monte Carlo analyzes are chosen for statistical hypothesis testing in the following validation phase (Section 4.2). Instead of comparing the residuals with the expected behavior of a normal distribution, these analyzes directly simulate the effect of randomness by randomly re-arranging the data and recalculating regression characteristics (e.g., slope and intercept) a representative number of times, usually 1,000 or more [69,70]. However, it is worth noting that some critics have been raised on the use of Monte Carlo methods to estimate P-values for statistical hypothesis testing [71].

4.2. Efficiency models candidates: statistical validation

The intention of the work presented in this section is to test the selected Efficiency models candidates (ME1b, ME1c, and ME3b) with a group of WTs which are different from the ones used for establishing the models, namely the Testing set (see Section 3). To test their validity, the η values from the Testing set were plotted against the corresponding $\hat{\eta}$ estimates from the three candidates. Regression analyzes were performed from these plots and the deviations from an ideally expected behavior were calculated. Based on these results, the definitive η model was established as MED (Model of Efficiency in function of Diameter).

In an ideal scenario, there would be a complete correspondence between the *Predictor* variable X ($\hat{\eta}$ estimates from the models) and the *Response* variable Y (η values from the Testing set). A regression line fitted to the data would then have a slope of 1 and a Y-Intercept of 0. In other words, $X = Y$. This perfectly linear correlation, where all the Y variance would be explained by the variance in X, would result in $r = 1$ and $R^2 = 1$. The RMSE would tend to zero. Moreover, Monte Carlo analyzes to test the significance of the regression [69], i.e., statistical hypothesis tests on the slopes, would be expected to result in significantly low P-values. Manly [70] suggests a minimum of 1,000 Monte Carlo simulations for randomization tests when a 5% significance level is used. In this work, a number of 100,000 simulations is used for all Monte Carlo analyzes performed.

Having established the ideal scenario, it can be used as a reference for comparing the results obtained for the Efficiency models candidates. The intention is to assess whether the deviations from this scenario are statistically significant and whether the models lead to better estimates as opposed to just using η_R directly ($\hat{\eta} = \eta_R$) or assuming an average efficiency ($\hat{\eta} = \bar{\eta}$) regardless of the nominal specifications. $\bar{\eta}$ is the *Mean Total Efficiency* among the WTs in the Training set, which resulted in $\bar{\eta} = 0.4147$. Fig. 9 and Table 3 present the Regression results of analyzing the η values from the Testing set plotted against estimates from: the three models candidates, the η_R values from the Testing set, and $\bar{\eta}$.

From Table 3, it can be seen that the performance of the three candidates was almost identical. This is also evidenced in Fig. 9(a), (c), and (e), where the dotted regression lines of the three models closely approach the ideal $X = Y$ line. This is evidenced visually as well as with the presented slopes close to 1 and the intercepts close to 0. Moreover, the Monte Carlo randomization analyzes on the significance of the regressions [69] resulted extremely statistically significant with P-values tending to 0 for the three models. This means that in none of the Monte Carlo data re-arrangements a regression slope was equal or greater than the absolute value of the slopes observed in Fig. 9(a), (c), and (e). Therefore, it is assumed that the observed linear responses of η, in the

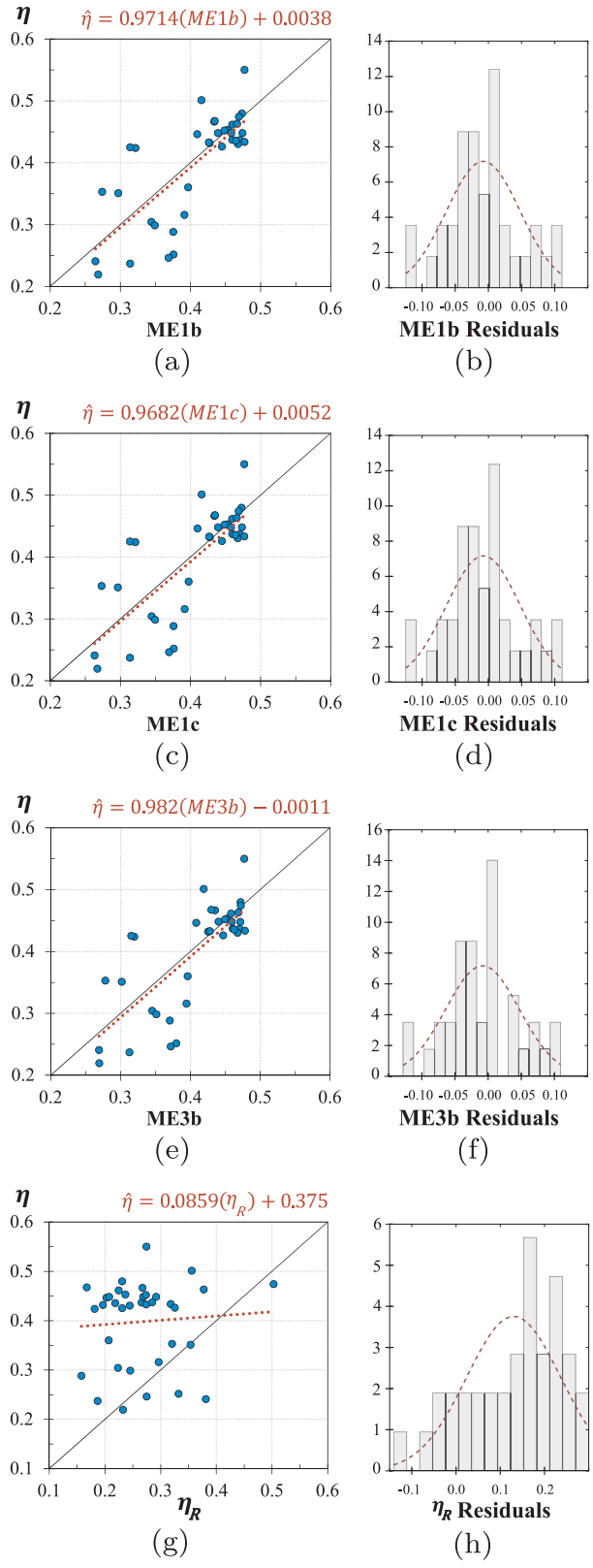

Fig. 9. Regression analyzes of the η models in the validation tests for (a)-(b) ME1b, (c)-(d) ME1c, (e)-(f) ME3b, and (g)-(h) η_R.

Table 3
Regression results of the η values from the Testing set plotted against modeled estimates.

	ME1b	ME1c	ME3b	η_R	$\bar{\eta}$
r	0.758	0.757	0.757	0.070	-
R^2	0.574	0.573	0.573	0.005	-
Slope P-value	0	0	0	0.685	-
RMSE	0.0562	0.0563	0.0563	0.1681	0.0868

three models candidates, are related to the corresponding estimates and not caused by randomness alone.

ME1b achieved the best estimation performance, with the highest r and R^2, and the lowest RMSE. Conversely, the regression line for η_R (in 9(g)) considerably deviates from the ideal behavior. It is worth noting that using η_R to directly estimate $\hat{\eta}$ resulted in an even higher RMSE compared to just assuming a fixed $\bar{\eta}$ for all WTs (see Table 3). Furthermore, the Monte Carlo significance of regression test for η_R resulted in a non-significant P-value that is in agreement with the weak linear response observed in Fig. 9(g).

It is also of interest to analyze the behavior of the Estimation Residuals from the previous validation tests. With Residuals defined as the η values from the Testing set minus the corresponding estimates ($\hat{\eta}$). Ideally, when plotted against the estimates, the Residuals would be randomly (normally) distributed around a regression line with slope and Y-Intercept of 0. In other words, no significant central linear trend should be observed in the Residuals. This behavior was tested in Table 4 with Shapiro-Wilk tests to evaluate normality and with Monte Carlo randomization analyzes [69] to evaluate the significance of the slopes and intercepts observed in the Residuals. The distributions of the Residuals are presented in Fig. 9(b), (d), (f), and (h) for ME1b, ME1c, ME3b, and η_R, respectively.

Even though no Shapiro-Wilk test result revealed significant violations to normality, from Fig. 9(h) it is visually evident that the Residuals from η_R deviate from the normal behavior. Moreover, the Slope and Intercept P-values reveal that there is a significant linear trend within the Residuals from η_R.

On the other hand, none of the Efficiency models candidates presented significant results in Table 4. This implies that their estimation errors may be assumed as approximately random. Also, any linear trends present in their Residuals can probably be explained by randomness as opposed to systematic errors introduced by the models. As mentioned in Section 3, it is worth emphasizing that, while there is no evidence of systematic errors in the candidates, they were constructed and tested within a dataset that may or may not be biased.

Based on the testing results presented in this subsection, ME1b is selected as the definitive Efficiency model. From this point, it will be referred to as MED (Model of Efficiency in function of Diameter). This is established in Eq. (3) with the hyperparameters stated in Table 2 and the fitted parameters shown in Fig. 8(a).

$$MED = \hat{\eta} = 4.12265D^{1/100} - 3.85416 \tag{3}$$

As compared to the other candidates, MED presented the highest correlation (in terms of r), the strongest linear response (in terms of R^2 and the regression slope P-value) and the smallest estimation error (in terms of RMSE). Also, the linear trend of its estimation Residuals did not evidence a significant deviation from the ideal behavior. Moreover, the results suggest that MED is more useful for estimating $\hat{\eta}$ as opposed to using η_R or $\bar{\eta}$ directly.

4.3. Established Efficiency model: uncertainty analysis

While MED allows estimating $\hat{\eta}$, it is a statistical model based on observed trends from a subset of the entire possible population. It is not based on physical causal relations. Therefore, considerable deviations are expected for particular applied cases where the model is used to estimate the $\hat{\eta}$ of a given WT. This section presents two proposed approaches that can be used for assessing the uncertainty that using MED entails: *Prediction Intervals* (PI) and *Stochastic Dominance*. As explained in Section 4.1, the Residuals from MED do not meet the parametric assumptions, so both approaches are analyzed through Monte Carlo methods [70,69].

When MED is used for estimating $\hat{\eta}$ values of WTs outside the dataset of this study, additional uncertainty is introduced in the estimates. This spreads further the distribution of possible values around $\hat{\eta}$. If MED is applied to new data, Prediction Intervals can provide a range where the actual η values are expected to fall with a given probability. In this work, the Monte Carlo method Bootstrapping [72] is used to characterize the 95% Prediction Intervals for MED. The resulting limits of these intervals are presented in Fig. 10.

The upper limit of the 95% PI (η_{95high}) is, on average, 0.1008 above the MED $\hat{\eta}$ estimates, while the lower limit (η_{95low}) is, on average, 0.114 below. The Bootstrapping method was used to numerically estimate the $\hat{\eta}$ values for the upper and lower 95% limits at regular intervals in the X-axis (using $X = D^{0.01}$). By fitting Linear Regression models to these values, it was possible to describe $\widehat{\eta_{95high}}$ with Eq. (4) and $\widehat{\eta_{95low}}$ with Eq. (5). These regression models characterize the upper and lower 95% PI with high fidelity, achieving $R^2 > 0.999$ in both cases.

$$\widehat{\eta_{95high}} = 4.05181D^{1/100} - 3.68091 \tag{4}$$

$$\widehat{\eta_{95low}} = 4.16546D^{1/100} - 4.01204 \tag{5}$$

Fig. 10 shows the data used to establish MED (Training data) as well as the data used to validate it (Testing data). The Testing data visually appear to follow the general trend predicted by MED. Of the 36 WTs from the Testing set, 4 (the 11%) were outside the 95% PI. However, these values outside the expected range had, on average, a distance from the corresponding 95% PI limits of just 2.5% of their magnitude. This suggests that the established intervals in Eqs. (4) and (5) provide a reasonable estimation of the range where the η of most WTs would probably fall.

The Betz limit states that no wind turbine can surpass a maximum theoretical efficiency of $\eta \approx 0.593$ [4]. In Fig. 11, MED, $\widehat{\eta_{95high}}$ and $\widehat{\eta_{95low}}$ are extrapolated to assess their intersection with the Betz limit. It was found that the MED estimates cross this barrier when $D > 1{,}952.7$ m, which is an unreasonable rotor diameter. Therefore, for WTs with a feasible size, MED does not violate this law and is consistent with the known physical and technical limits. $\widehat{\eta_{95low}}$ crosses Betz for far larger WTs, i.e., $D > 22{,}711.7$ m. However, $\widehat{\eta_{95high}}$ crosses it when $D > 207.8$ m, a size that could be reached in future wind energy developments [18]. Hence, it is worth noting that all estimations with MED, $\widehat{\eta_{95high}}$ and $\widehat{\eta_{95low}}$ should be limited as $0 \leq \hat{\eta} \leq 0.593$.

As MED is a statistical model, its $\hat{\eta}$ estimates do not refer to specific WTs. Instead, a particular estimate refers to the expected mean of a distributed population of potential WTs with the same rotor diameter used as input for the model. Therefore, the actual η of a particular WT may be any of the values from such a potential population and not necessarily the estimated mean delivered by the model. This introduces an important uncertainty when it comes to establishing ranks for selecting among particular WTs.

For instance, with two WTs being compared, their diameters may be used in MED to estimate $\hat{\eta}$ and determine which turbine is expected to be more efficient. According to MED, the turbine with the largest diameter is expected to have the greatest efficiency. However, the actual η

Table 4
Inferential results of the $\hat{\eta}$ Estimation Residuals.

Residuals from:	ME1b	ME1c	ME3b	η_R
Shapiro-Wilk	0.514	0.495	0.546	0.098
Slope P-value	0.844	0.826	0.903	8E-5
Intercept P-value	0.949	0.929	0.986	0

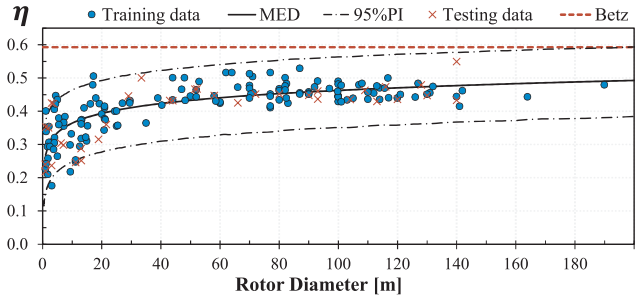

Fig. 10. 95% Prediction Intervals for the MED η model.

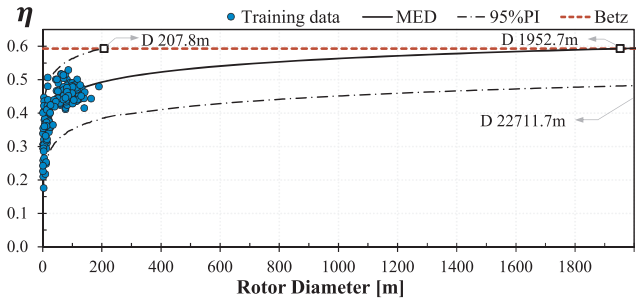

Fig. 11. MED and 95% PI extrapolations compared to Betz limit.

for both turbines can be any value corresponding to the potential populations distributed around the MED estimates. Consequently, even though the $\hat{\eta}$ estimates may rank a given turbine over another one, the actual η values may have the opposite rank. It is reasonable to assert that, the larger the difference between two $\hat{\eta}$ estimates, the more likely it is that the expected rank corresponds to the actual rank. Conversely, the smaller the *Absolute Delta in Estimated Efficiency* ($|\Delta\hat{\eta}|$), the more uncertainty associated with the estimated rank. This is related to the concept of *Stochastic Dominance*, namely "The probability that a randomly drawn observation from one group will be greater than a randomly drawn observation from another" [73].

The concept of stochastic dominance is critical in the aim of this work for developing a selection method based on ranking WTs from statistical estimations. How much can the users of the method trust in the ranks suggested by MED? To address this query, a Monte Carlo method was developed based on basic randomization principles [70].

This method assesses the probability that a given estimated rank is opposite to the actual rank as a function of $|\Delta\hat{\eta}|$. The proposed method makes use of the populations of simulated values created in the Bootstrapping analysis [72] for the 95% Prediction Intervals. The proposed Steps to calculate the probability that the estimated $\hat{\eta}$ rank gets inverted for two given WTs, are described as follows:

1. Through Bootstrapping, populations of simulated $\hat{\eta}$ values are created for a representative range of rotor diameters. These populations of potential WTs consider the expected variability and uncertainty related to making inferences from a sample as well as the uncertainty related to making $\hat{\eta}$ estimates for turbines which were not used to train MED.
2. A representative number of WT pairs is randomly selected from the given range of rotor diameters. In this study, 100 pairs were established, each containing two randomly assigned rotor diameters. These pairs represent potential cases where two particular WTs with different D are compared. Another number of pairs may be established, but 100 was effective for encompassing the range of possible $|\Delta\hat{\eta}|$ values with a smooth behavior.
3. For every D in the established pairs, the $\hat{\eta}$ value is estimated with MED. For every representative pair, the estimated rank is established and $|\Delta\hat{\eta}|$ can then be calculated.

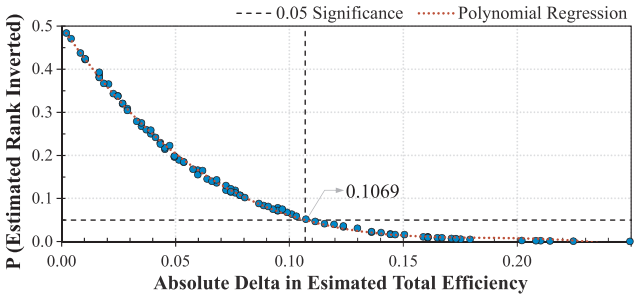

Fig. 12. Analysis of the Stochastic Rank Dominance in terms of $|\Delta\hat{\eta}|$.

4. For every D in the established pairs, there is a corresponding population of simulated $\hat{\eta}$ values from Step 1. For every pair, two individuals are randomly drawn from the corresponding $\hat{\eta}$ simulated populations and it is checked whether their actual rank is the opposite of the originally estimated rank ($|\Delta\hat{\eta}|$). In accordance with a Monte Carlo randomization approach [70], this stochastic process is repeated a representative number of times for every pair, in this case, 100,000 times. The probability that $|\Delta\hat{\eta}|$ gets inverted with the actual η values of a given WTs pair ($P_{\Delta\hat{\eta}\,invert}$) is calculated as: the number of times the estimated rank was inverted over the 100,000 random sampling individual selections. This results in a series of $P_{\Delta\hat{\eta}\,invert}$ values related to 100 $|\Delta\hat{\eta}|$ values.
5. Lastly, the trend of $P_{\Delta\hat{\eta}\,invert}$ in function of $|\Delta\hat{\eta}|$ is characterized through a Regression model.

Fig. 12 presents the result after implementing the previously proposed Steps 1–5. The figure illustrates the behavior of $P_{\Delta\hat{\eta}\,invert}$ in function of $|\Delta\hat{\eta}|$. To characterize this evidently consistent and smooth trend, a Polynomial Regression model was fitted (Eq. (6)), achieving a satisfactorily low $RMSE = 0.0048$.

The lower $\widehat{P_{\Delta\hat{\eta}\,invert}}$ is, the less likely it is that the rank obtained from MED estimates is different from the actual η rank for two particular WTs. As shown in Fig. 12, a 5% significance level is expected when $|\Delta\hat{\eta}| \geq 0.1069$.

$$\begin{aligned}\widehat{P_{\Delta\hat{\eta}\,invert}} &= -74.573\ |\Delta\hat{\eta}|^3 + 41.641\ |\Delta\hat{\eta}|^2 \\ &\quad - 7.8026\ |\Delta\hat{\eta}| + 0.4993 \\ &\approx 0, \quad \text{if } |\Delta\hat{\eta}| > 0.23\end{aligned} \tag{6}$$

In this subsection, two approaches were presented to assess the uncertainty of using MED for estimating the $\hat{\eta}$ of turbines which were not used in the construction of the statistical model. 95% Prediction Intervals can be estimated with Eqs. (4) and (5) to confine the expected uncertainty of the MED estimates within reasonable upper and lower limits. If two given turbines are being compared in terms of the estimated $\hat{\eta}$ rank, Eq. (6) can be used to estimate the probability that such rank gets inverted with the actual unknown η values.

5. Statistical modeling of the Hub height

The purpose of this section is to explore whether a valid statistical model for estimating tentatively feasible *Hh* values (see Section 3) can be established in function of variables obtained from the nominal specifications. The independent variables D and η_R are first examined as possible modeling *Predictors*. Afterwards, only D is considered a valuable potential predictor. Following the same approach described in Section 4, a range of linearization transformations are applied to the predictor variable in Simple Linear Regression models fitted to the Training set. Among these models configurations, two Hub height models candidates are selected based on a 5-fold cross-validation evaluation. These candidates are fitted to the whole Training set and then statistically evaluated in the Testing set. The model with the best estimation performance is established as MHhD (Model of Hub height in

function of Diameter). Finally, MHhD is further explored in terms of the uncertainty involved in estimating $\widehat{Hh}$ for WTs outside the Training set. The relevant programming languages and packages used for the statistical procedures are described at the beginning of Section 4.

5.1. Hub height models candidates: modeling

In this subsection, potential statistical models of *Hh* (*Response variable Y*) are systematically explored. For clarification on the procedures performed, refer to Section 4.1 as the same statistical analyzes are used. It must be noticed that the regression models of this exploration do not assume direct causality regarding *Hh*. These models intend to analyze whether simple and easily-available nominal variables can be of any use in the estimation of $\widehat{Hh}$.

The variables D and η_R are first examined before establishing the modeling *Predictors*. Fig. 13(a) illustrates a clear response of *Hh* in function of *D*. As a slight "bulge" is evidenced in the data distribution, the linear behavior of the data may be effectively improved by Tukey's Ladder of powers [66]. Conversely, the data in Fig. 13(b) does not reveal a clear trend of any kind. Also, the data distribution does not evidence a "bulge" that may be linearized.

To further inspect the suitability of n_R as a predictor, a Linear Regression analysis was performed. The resulting parameters are shown in Fig. 13(b). As the Residuals presented violations to Normality (Shapiro-Wilk P-value = 0.001), a Monte Carlo analysis was used to test the significance of the regression (related to the observed Slope). This resulted in a non-significant P-value = 0.2002. Thus, there is not enough evidence to suppose that the observed Slope is not caused by randomness alone. Consequently, only *D* is established as *Predictor* and the analysis is defined as:

- MHh: $\widehat{Hh} = f_{(D)}$. The Hub height is estimated as a function of the rotor Diameter.

The linearization procedure (Tukey's Ladder of powers [66]) of *D* as predictor was performed by iterating λ from -3 to 3 in steps of 0.01. Every λ value was evaluated through a 5-fold cross-validation analysis [32]. The corresponding results are illustrated in Fig. 14, where the mean *Coefficient of Determination* ($\overline{R^2}$), mean *Pearson's Coefficient* ($\bar{r}$), and mean *Root Mean Square Error* ($\overline{RMSE}$) were calculated. The points where every performance curve was optimized were highlighted in the figure as points of interest (b, c).

Table 5 presents the results for the points of interest in the MHh analysis. Also, the performance of the untransformed predictor variable (Row a) is presented, which can be used as a comparison reference and to understand the impact of the linearization procedure. The improvement of MHhb and MHhc over MHha, in terms of $\bar{r}$, $\overline{R^2}$, and $\overline{RMSE}$, suggests that the linearization procedure was effective.

MHhb and MHhc were selected as the Hub height models candidates. The two models were fitted to the whole Training set to obtain the corresponding parameters, i.e., the slopes and intercepts. This is shown in Fig. 15. In both subfigures, the response of *Hh* in function of the transformed predictors can be visually identified as linear, which is also supported by the high $\bar{r}$ values presented in Table 5. Therefore, no further non-linear regression analyzes will be performed.

The residuals from the fitted regression models (Fig. 15) were tested for normality with Shapiro-Wilk analyzes, resulting in P-value = 0.0348 for MHhb and P-value = 0.0275 for MHhc. These violations to Normality were expected due to the fact that *D* is not the only factor influencing the average *Hh* from towers commercially available. Nonetheless, this is an acceptable limitation within the framework of this work as the objective is to define the model in function of only variables that can be obtained from nominal specifications. Hence, Monte Carlo analyzes are chosen for statistical hypothesis testing in the following validation phase (Section 5.2).

Seeking to gain a deeper insight into the relation between *Hh* and *D*, Fig. 16 plots the Relative *Hh* (*Hh*/D) in function of the rotor diameter. The mean Relative *Hh* was 1.57%. Loosely speaking, this means that the tower's height tends to be 57% larger than the diameter of a corresponding turbine. However, this proportion presents an evidently decreasing trend. This makes intuitive sense because the gain in wind strength due to increased height presents diminishing returns. For instance, a turbine with $D = 5$ m should ideally be several times its diameter above the ground for it to avoid the worst effects of turbulence and ground friction. Conversely, average winds do not necessarily improve above the lower atmospheric layer (150–200 m above ground level) [23]. Hence, for WTs with $D > 100$ m, there is not necessarily a good incentive for considering towers larger than their diameter. Furthermore, it was found that both variables tend to be equal ($Hh = D$) around $D = 80$ m.

5.2. Hub height models candidates: statistical validation

The purpose of the work presented in this section is to test the selected Hub height models candidates (MHhb and MHhc) with a group of WTs which are different from the ones used for establishing the models, namely the Testing set (see Section 3). To test their validity, the *Hh* values from the Testing set were plotted against the corresponding $\widehat{Hh}$ estimates from the two candidates. Simple Linear Regression analyzes were performed from these plots and the deviations from an ideally expected behavior (described in Section 4.2) were calculated. The intention is to assess whether the deviations from this scenario are statistically significant and whether the models lead to better estimates as opposed to just using the mean Relative *Hh* calculated in Section 5.1. Based on these results, the definitive *Hh* model was established as MHhD (Model of Hub height in function of Diameter).

Fig. 17 and Table 6 present the Regression results of analyzing the *Hh* values from the Testing set plotted against estimates from: the two candidate models and from the Relative *Hh*. In the latter, referred to as RHh, the estimates correspond to the mean Relative *Hh* multiplied by the diameters in the Testing set.

From Table 6, the evaluated results from the three models are very similar except for the RMSE of RHh, which was almost six times larger than the other two. This difference is illustrated in Fig. 17(e), where a clear trend diverges from the ideal behavior shown by the line ($X = Y$). Conversely, Fig. 17(a) and (c) show how the dotted regression lines of

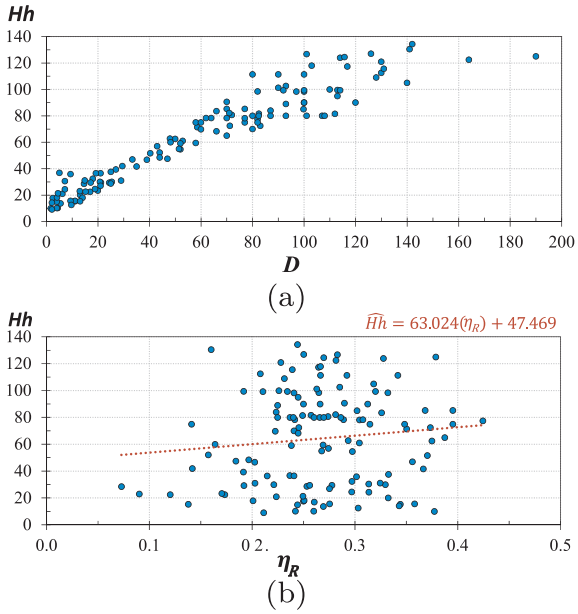

Fig. 13. Response variable *Hh* plotted against potential predictors *D*, in (a), and η_R, in (b).

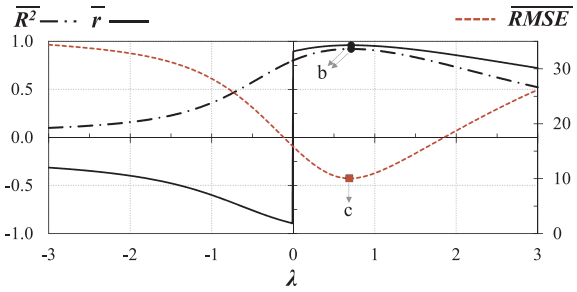

Fig. 14. Cross-validation evaluation of Tukey's Ladder of powers, iterating λ for D^{λ}.

Table 5
Points of interest in the cross-validation evaluation of Tukey's Ladder of powers, iterating λ for D^{λ}.

	X	$\overline{r}$	$\overline{R^2}$	$\overline{RMSE}$
a	D	0.95178	0.905896	10.98926
b	$D^{0.71}$	0.95950	0.920659	10.04665
c	$D^{0.69}$	0.95948	0.920611	10.04407

The results with the best performance are underlined.

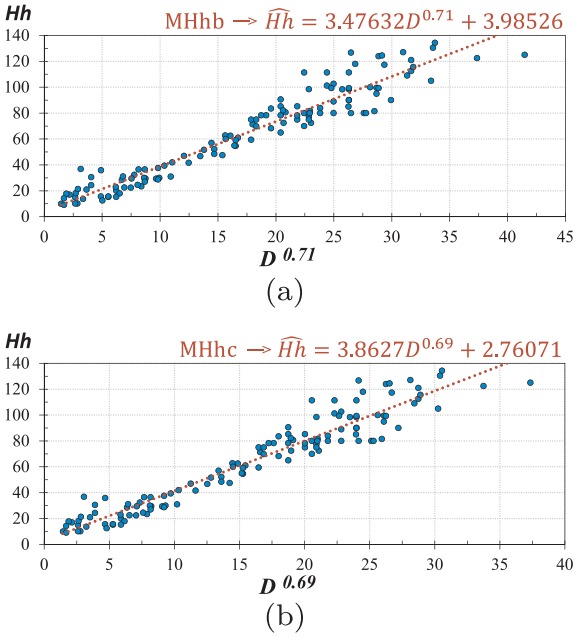

Fig. 15. Hub height models candidates fitted to the whole Training set: MHhb in (a) and MHhc in (b).

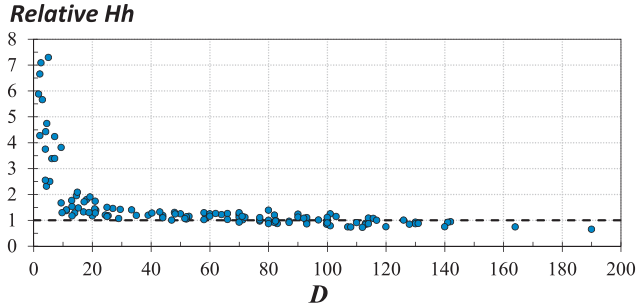

Fig. 16. Relative *Hh* in function of *D*.

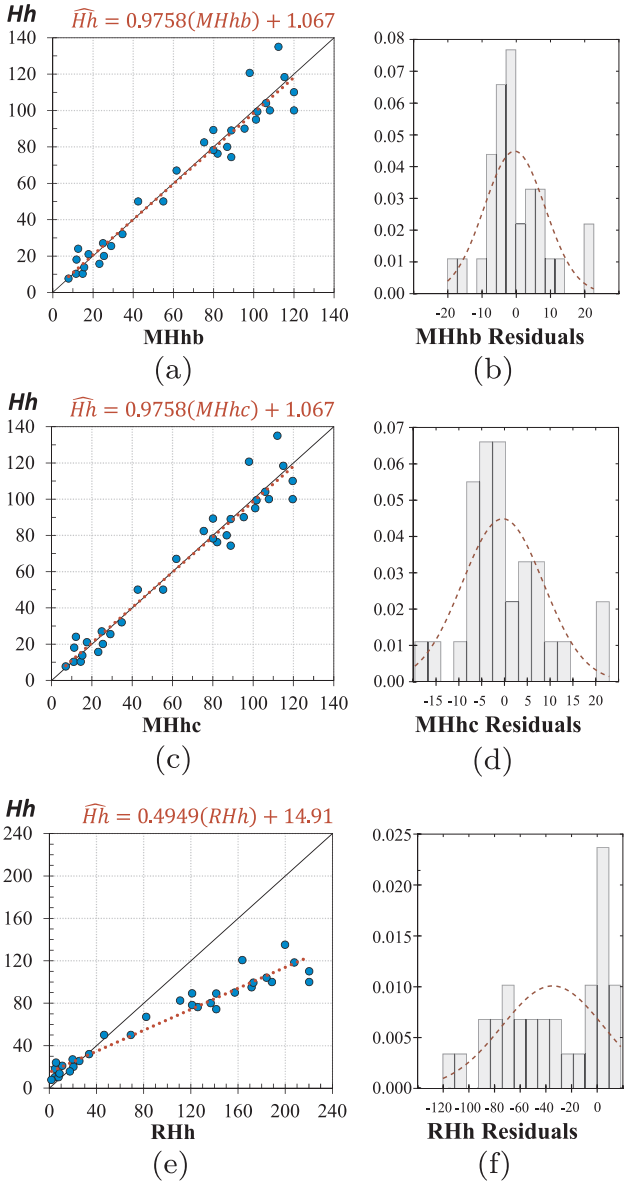

Fig. 17. Regression analyzes of the *Hh* models in the validation tests for (a)-(b) MHhb, (c)-(d) MHhc, and (e)-(f) RHh.

Table 6
Regression results of the *Hh* values from the Testing set plotted against modeled estimates.

	MHhb	MHhc	RHh
r	0.9737	0.9738	0.9676
R^2	0.9482	0.9483	0.9362
Slope P-value	0	0	0
RMSE	8.9087	8.9011	52.674

the two models candidates closely approach the expected trend. This is further evidenced by the presented slopes close to 1 and the intercepts close to 0. As all the Monte Carlo tests on the significance of the Slopes resulted in *P*-values tending to 0, it is assumed that the three observed linear responses are related to the corresponding estimates and not caused by randomness alone.

The behavior of the Estimation Residuals from the previous validation tests is addressed in Table 7. From the Shapiro-Wilk results and the histograms in Fig. 17, it can be seen that the Residuals from RHh

Table 7
Inferential results of the $\widehat{Hh}$ Estimation Residuals.

Residuals from:	MHhb	MHhc	RHh
Shapiro-Wilk	0.075	0.076	0.016
Slope P-value	0.569	0.542	0
Intercept P-value	0.694	0.638	0.106

presented clear violations to Normality. Also, the linear trend in these Residuals presented significant results in terms of its Slope P-value. On the other hand, none of the Hub height models candidates presented significant results in Table 7. This implies that their estimation errors may be assumed as approximately random and there is no evidence of systematic errors introduced by the models candidates.

Based on the testing results presented in this subsection, MHhc is selected as the definitive Efficiency model. It presented the highest r and R^2, and the lowest RMSE. The results also suggest that the selected model is more useful for estimating $\widehat{Hh}$ as opposed to using the mean Relative *Hh* directly. From this point, it will be referred to as MHhD (Model of Hub height in function of Diameter). This is established in Eq. (7) with the hyperparameters stated in Table 5 and the fitted parameters shown in Fig. 15(b).

$$MHhD = \widehat{Hh} = 3.8627D^{0.69} + 2.76071 \tag{7}$$

Although the linear trend of the estimation Residuals of MHhD did not evidence a significant deviation, it is important to emphasize that it was constructed and tested within a dataset that may or may not be biased (see Section 3).

5.3. Established Hub height model: uncertainty analysis

MHhD is a statistical model based on observed trends from a subset of the entire possible population. Thus, considerable deviations are expected for particular applied cases where the model is used to estimate the $\widehat{Hh}$ of a given WT. As in Section 4.3, this subsection presents two proposed approaches that can be used for assessing the uncertainty that using MHhD entails: *Prediction Intervals* (PI) and *Stochastic Dominance*.

When MHhD is applied for estimating $\widehat{Hh}$ values of WTs outside the dataset of this study, Prediction Intervals can provide a range where the actual *Hh* values are expected to fall with a given probability (95% is used in this study). The Monte Carlo method Bootstrapping [72] is used in this work to characterize the 95% PI (shown in Fig. 18).

The upper limit (Hh_{95high}) is, on average, 22.22 m above the MHhD $\widehat{Hh}$ estimates, while the lower limit (Hh_{95low}) is, on average, 19.63 m below. By fitting Linear Regression models to the limiting values obtained from the Bootstrapping method, it was possible to describe $\widehat{Hh_{95high}}$ with Eq. (8) and $\widehat{Hh_{95low}}$ with Eq. (9). These regression models characterize the upper and lower 95% prediction limits with a high fidelity of $R^2 > 0.9999$ in both cases.

$$\widehat{Hh_{95high}} = 3.8644D^{0.69} + 24.9449 \tag{8}$$

$$\widehat{Hh_{95low}} = 3.82633D^{0.69} - 16.12461 \tag{9}$$

Fig. 18 shows the data used to establish MHhD (Training data) as well as the data used to validate it (Testing data). The Testing data appear to follow the general trend predicted by MHhD. Of the 32 WTs used for validation from the Testing set, only 2 (the 6.3%) were outside the estimated 95% PI. Moreover, these *Hh* values had, on average, a distance from the corresponding 95% PI limits of just 0.44% of their magnitude. This suggests that the established intervals in Eqs. (8) and (9) provide a reasonable estimation of the range where the *Hh* corresponding to most WTs would probably fall.

A particular MHhD estimate refers to the expected mean of a distributed population of potential WTs with the same rotor diameter used as modeling input. Consequently, even though $\widehat{Hh}$ estimates may rank a given turbine over another one, the actual *Hh* values may have the opposite rank. For two WTs being compared, the smaller the *Absolute Delta in Hub-height* ($|\Delta\widehat{Hh}|$), the more uncertainty associated with the estimated rank. This is related to the concept of *Stochastic Dominance* [73]. As discussed in Section 4.3, this work proposes a Monte Carlo method that can be applied to address the query: How much can the ranks estimated by MHhD be trusted? This method assesses the probability that the estimated rank is opposite to the actual rank as a function of $|\Delta\widehat{Hh}|$. Fig. 19 presents the result after implementing the proposed method. The figure illustrates the behavior of $P_{\Delta\widehat{Hh}invert}$ in function of $|\Delta\widehat{Hh}|$.

The data in Fig. 19 follows an evidently consistent and smooth trend. To characterize this central behavior, a Polynomial Regression model was fitted (Eq. (10)) with a satisfactorily low $RMSE = 0.0027$.

$$\begin{aligned}\widehat{P_{\Delta\widehat{Hh}invert}} &= -6.745\text{E}{-6}\ |\Delta\widehat{Hh}|^3 + 8.476\text{E}{-4}\ |\Delta\widehat{Hh}|^2 \\ &\quad - 0.03572\ |\Delta\widehat{Hh}| + 0.5078 \\ &\approx 0, \quad \text{if } |\Delta\widehat{Hh}| > 48\end{aligned} \tag{10}$$

The lower $\widehat{P_{\Delta\widehat{Hh}invert}}$ is, the less likely it is that the rank obtained from MHhD estimates is different from the actual *Hh* rank for two particular WTs. As shown in Fig. 19, a 5% significance level is expected when $|\Delta\widehat{Hh}| \geq 23.35$.

In this subsection, two approaches were presented to assess the uncertainty of using MHhD for estimating the $\widehat{Hh}$ of turbines which were not used in the construction of the statistical model. 95% Prediction Intervals can be estimated with Eqs. (8) and (9) to confine the expected uncertainty of the MHhD estimates within reasonable upper and lower limits. For two given turbines being compared in terms of the estimated $\widehat{Hh}$ rank, Eq. (10) can be used to estimate the probability that such rank gets inverted with the actual unknown *Hh* values.

6. Proposal of a wind turbine selection method

In this section, a new method for comparing and selecting HAWT turbines is proposed. The steps of the method, presented in Fig. 20, are based on the statistical models established and validated in Sections 4 and 5 as well as on wind speed extrapolation, energy and cost models taken from the relevant literature (discussed throughout the section). For instance, the models JM (Justus and Mikhail) [23] and SR (Spera and Richards) [74] are used in Step 5 for extrapolating the Weibull parameters to the Hub height.

Each step is explained in detail in Sections 6.1–6.5. With this method, the turbines are compared by ultimately estimating the overall cost of energy. This variable depends on a plurality of detailed technical and weather-related factors which are not always easily accessible and trustworthy. As presented in Section 2, a common applied problem is when non-experts must select among commercial wind turbines with only nominal specifications and a standard characterization of the local wind conditions at hand. Facing this need, the method proposed in this section provides the means for a preliminary selection. This preliminary selection process can help narrow down the WT choices for further

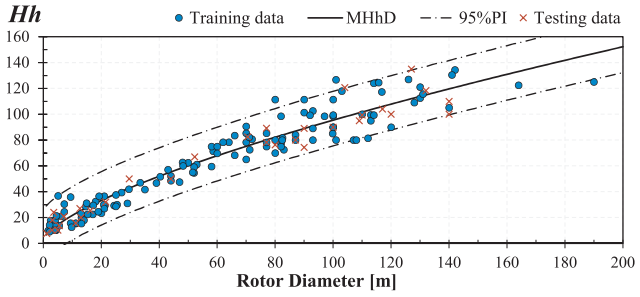

Fig. 18. 95% Prediction Intervals for the MHhD model.

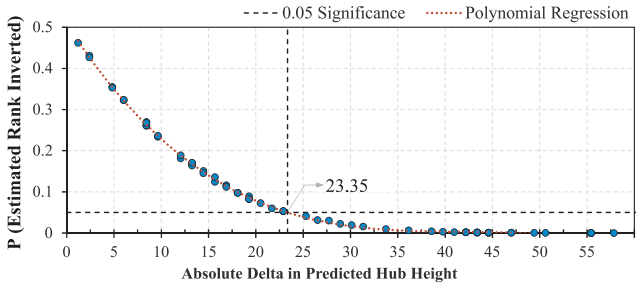

Fig. 19. Significance analysis of the Stochastic Rank Dominance in terms of $|\Delta\widehat{Hh}|$.

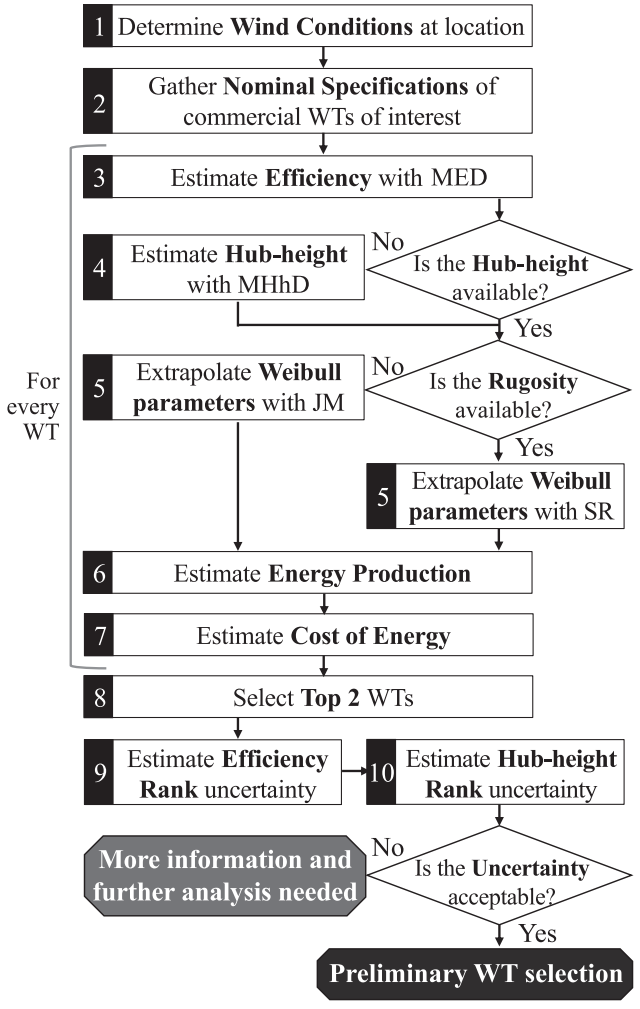

Fig. 20. Proposed wind turbine selection method.

more detailed analyzes or may empower a final selection if no other means are accessible.

6.1. Input information

The first two steps of the method (Fig. 20) comprise the indications for gathering the inputs required. Step 1 is to determine the variables that characterize the local wind conditions where the WTs are supposed to be installed: the *Air Density* (ρ) in [kg/m^3], the Weibull *Shape* ($k1$) and *Scale* ($c1$) parameters measured at a height $h1$ in [m] above the ground, and the *Surface Roughness* (Z_0) in [m].

ρ can be assumed as the standard air density at sea level (1.225 kg/m^3). On the other hand, it can be calculated in function of the *Height Above Sea Level* (h_{asl}), in [m], with the International Standard Atmosphere model [75] (Eqs. (11)–(13)).

$$\rho = \frac{p}{287.04T} \tag{11}$$

Where the *Air Pressure* (p) in [Pa] and the *Air Temperature* (T) in [K] at h_{asl} can be estimated with:

$$p = 101{,}325\left[1-\frac{0.0065h_{asl}}{288.15}\right]^{5.2561} \tag{12}$$

$$T = 288.15-0.0065h_{asl} \tag{13}$$

In terms of the Weibull parameters, the Shape (k) is usually assumed to be 2 when it has not yet been established for the particular location [76]. If the Scale ($c1$) is not available once $k1$ has been established, it can be calculated from the *Average Wind Speed* ($\overline{V}$) [m/s] with Eq. (14).

$$c1 = \frac{\overline{V}}{\Gamma(1 + 1/k1)} \tag{14}$$

On the other hand, if $k1$ and $c1$ have not been calculated yet, but there is detailed information about the wind speed frequencies or direct instantaneous measurements throughout a representative period of time, Seguro and Lambert [76] present several methods that can be used for estimating the Weibull parameters. It is worth noting that both $k1$ and $c1$ must be directly related to a known height above the ground level ($h1$). As wind speed is usually measured at $h1 = 10$ m [22], the Weibull parameters must be extrapolated to the Hub height whenever $Hh \neq h1$.

A representative *Surface Roughness* (Z_0) of the intended location is a useful input to better characterize the wind speed conditions, as the friction with the ground affects the wind's vertical profile. Hence, Z_0 conditions the way in which the wind speeds are expected to behave at a height different from $h1$. Nonetheless, as explained in Section 6.2, this wind speed extrapolation can also be performed without Z_0. Therefore, if this input is not available and trustworthy, it is not strictly required. On the other hand, the *Surface Roughness* can be taken from published tables [77,78], where different Z_0 values are associated with several kinds of terrains.

Step 2 is to gather the needed nominal specifications of the potential wind turbines that are available commercially and subject to be chosen in the applied problem: *Rotor Diameter* (D) in [m], *Hub height* (Hh) in [m], *Wind Turbine's Cost* (C_{wt}) in [USD], *Rated Power* (P_R) in [W], *Cut-in Speed* (V_{in}) in [m/s], *Cut-out Speed* (V_{out}) in [m/s], and *Lifespan* ($Life$) in [years].

If there is trustworthy information regarding the tower heights commercially offered for a given WT, Hh can be taken as the average between them. Otherwise, Hh can be estimated in Step 4. On the other hand, D and C_{wt} are critical nominal inputs. Nonetheless, Mathew [40] provides an approach for making general C_{wt} estimates in function of P_R (Eq. (15)). This can be useful for more generic or broad comparisons.

$$C_{wt} = \begin{cases} 2.7P_R, & \text{if } P_R \leq 10{,}000 \\ 1.625P_R, & \text{if } 10{,}000 < P_R < 250{,}000 \\ 0.85P_R, & \text{if } P_R \geq 250{,}000 \end{cases} \tag{15}$$

If the available P_R is apparently misleading, it can be estimated with the modeled trend found in Section 3 (Eq. (2)). Also, for every WT, it must be established whether their power output is limited up to P_R, as discussed in Section 2 and illustrated in Fig. 2. Lastly, if the expected *Lifespan* is unknown, it can be taken as $Life = 20$ years, which is usually assumed in wind energy applications [79].

6.2. Efficiency and wind conditions at Hub height

Steps 3–5 go from estimating the *Total Efficiency* ($\hat{\eta}$) of the turbines considered to characterizing the wind conditions at Hh by extrapolating the Weibull parameters.

The $\hat{\eta}$ estimation in Step 3 can be performed with the proposed and validated MED model (Eq. (3)). Although using MED involves considerable uncertainty, the 95% Prediction Intervals, described by Eqs. (4) and (5) and illustrated in Fig. 10, provide a reasonable range where most η values are expected to fall. Similarly, the $\hat{Hh}$ estimation in Step 4 can be performed with the proposed and validated MHhD model (Eq. (7)) with the corresponding 95% Prediction Intervals described by Eqs. (8) and (9).

The estimation of $\hat{Hh}$ is key because it is usually different from the height at which the local wind conditions are characterized. Therefore, the Weibull parameters $k1$ and $c1$ need to be extrapolated to $k2$ and $c2$ at Hh in Step 5. As Fig. 20 indicates, if a trustworthy measurement of the rugosity of the terrain (Z_0) is available, the Spera and Richards [74,23,25] model (SR) can be used. $k2$ and $c2$ can then be calculated with Eqs. (16)–(19).

$$k2 = k1\left[\frac{1-\alpha_0 Ln(h1/10)/Ln(67)}{1-\alpha_0 Ln(Hh/10)/Ln(67)}\right] \tag{16}$$

$$c2 = c1\left(\frac{Hh}{h1}\right)^n \tag{17}$$

where

$$\alpha_0 = \left(\frac{Z_0}{10}\right)^{0.2} \tag{18}$$

$$n = \alpha_0\left[\frac{1-Ln(c1)/Ln(67)}{1-\alpha_0 Ln(h1/10)/Ln(67)}\right] \tag{19}$$

On the other hand, if Z_0 is not available, the Justus and Mikhail [23,80] model (JM) can be used. In this case, $c2$ is also calculated with Eq. (17) while $k2$ is defined by Eq. (20) and n by Eq. (21).

$$k2 = k1\left[\frac{1-0.0881 Ln(h1/10)}{1-0.0881 Ln(Hh/10)}\right] \tag{20}$$

$$n = \frac{0.37-0.0881 Ln(c1)}{1-0.0881 Ln(h1/10)} \tag{21}$$

Fig. 21(a) illustrates how the $k2$ and $c2$ parameters increase as they are extrapolated to higher Hh heights. In Fig. 21, SR is implemented with five different Z_0 values corresponding to representative kinds of terrains. These can be useful reference values for implementing the proposed method:

- $Z_0 = 0.0002$→ Water areas [77]
- $Z_0 = 0.01$→ Rough pasture [78]
- $Z_0 = 0.1$→ Farmland with closed appearance/Few trees [77,78]
- $Z_0 = 0.5$→ Forest and woodlands [78]
- $Z_0 = 1$→ Small town/Suburbs [77,78]

The JM curves are approximately central to the SR curves. As seen in the figure, the estimates of both extrapolation models resemble each other when $Z_0 = 0.1$. Fig. 21(b) illustrates the implications due to height extrapolation with the JM model on the Weibull distribution of wind speeds. The figure also presents the *Average Wind Speed* ($\overline{V}$) corresponding to each of the five frequency distributions. These examples show how increasing Hh implies decreasing speed gains. For instance, a 400% increment in height (from $h1 = 10$ m to $Hh = 50$ m) may imply a 42% gain in $\overline{V}$, while a 1400% increment in height (at $Hh = 150$ m) implies an 80% gain in $\overline{V}$.

6.3. Estimation of the Energy output

Step 6 consists in the calculations needed, for every potential wind turbine, to estimate the total *Energy output* (E) in [W h] with an expected lifespan. As shown in Fig. 22, the area below a regular power curve of a given WT can be divided into two main regions. The first one (E_0) extends from V_{in} to the *Rated Wind Speed* (V_R). The second region (E_R) characterizes the nominal behavior from V_R up to V_{out}.

V_{in} and V_{out} are established from Step 2. Although V_R is usually found within the nominal specifications, it is recommended to be calculated directly. In Section 2, it was illustrated with Fig. 2 how the nominal V_R can lead to a considerable mismatch between a (V_R, P_R) correspondence and a realistic power curve. Therefore, derived from Eq. (1), V_R can be directly estimated with Eq. (22).

$$V_R = \sqrt[3]{\frac{2P_R}{\rho A \eta}} \tag{22}$$

For calculating the area of E_0, the region is divided into nR Riemann rectangles of width V_Δ (Eq. (23)). The larger nR is, the better the accuracy and the smaller V_Δ becomes. Moreover, trapezoids may be used instead of rectangles to further improve the accuracy [81].

$$V_\Delta = \frac{V_R - V_{in}}{nR} \tag{23}$$

E_0 can then be estimated with Eq. (24), where each Riemann rectangle is represented by a given speed V_i located in the middle of its width V_Δ. The time t is the *Life* given in [h]. $f_{(Vi)}$ is the expected probability of occurrence for a given V_i speed, as indicated by a Weibull distribution of the wind conditions at Hh.

$$E_0 = \frac{1}{2}\rho A \eta t \sum_{i=1}^{r} V_i^3 f_{(Vi)} V_\Delta \tag{24}$$

where

$$V_i = V_{in} + \frac{V_\Delta}{2}(2i-1) \tag{25}$$

$$f_{(Vi)} = \frac{k2}{c2}\left(\frac{V_i}{c2}\right)^{k2-1} e^{-\left(\frac{V_i}{c2}\right)^{k2}} \tag{26}$$

E_R can be calculated with Eq. (27). What this equation conceptually does is to multiply the rated power by the total number of hours where the winds are expected to remain in the E_R region (see Fig. 22).

$$E_R = P_R t\left[F_{(V_{out})} - F_{(V_R)}\right] \tag{27}$$

where $F_{(x)}$ is the Weibull Cumulative distribution function:

$$F_{(x)} = 1 - e^{-\left(\frac{x}{c2}\right)^{k2}} \tag{28}$$

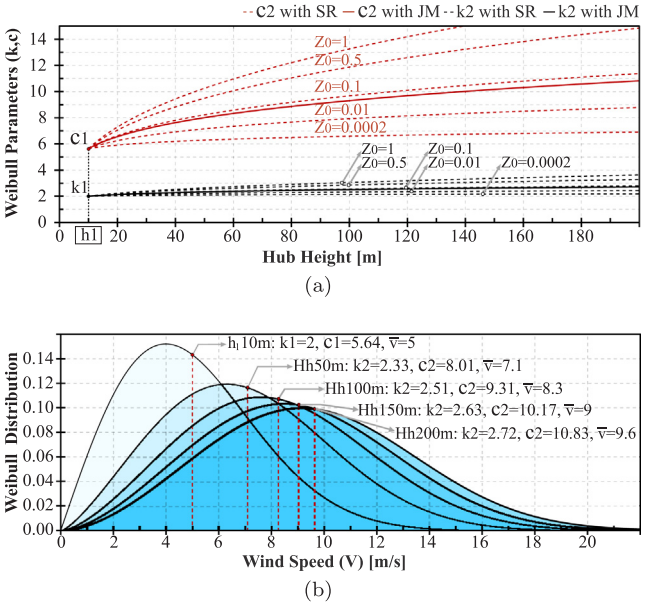

Fig. 21. Weibull parameters extrapolated with the SR and JM models.

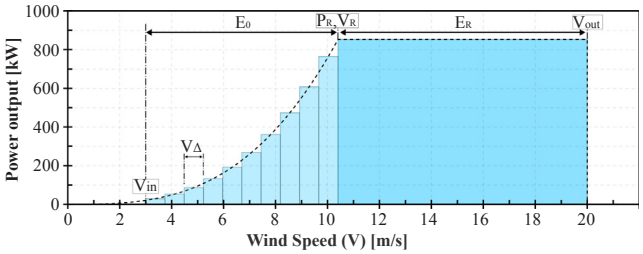

Fig. 22. Energy calculated from the Power Curve.

The *Total Energy output* (E) for an expected lifespan is then defined by Eq. (29). On the other hand, if the power output of a given WT is not limited to P_R (an input information in Step 2), then V_{out} is used instead of V_R and $E = E_0$.

$$E = E_0 + E_R \tag{29}$$

Fig. 23(a) shows an analysis of how E may behave for a range of rotor diameters. The description of this analysis and its continuation in Section 6.4 serves as an explicit guide and example on how to apply the proposed method for a generic assessment. Following the scheme from Fig. 20, the procedure was carried out up to Step 6 as follows:

- Step 1: ρ was calculated with Eqs. (11)–(13) for an altitude $h_{asl} = 0$ m. At $h1 = 10$ m, $k1$ was set to 2 and $c1$ was calculated with Eq. (14) for a $\overline{V} = 5$ m/s.
- Step 2: D was iterated in a range from 1 m to 200 m. P_R was generically estimated with Eq. (2) in function of every D. V_{in}, V_{out} and *Life* were set to 3 m/s, 20 m/s and 20 years, respectively.
- Step 3: η was estimated, in function of every D in the range, with the central efficiency MED model (Eq. (3)), as well as with the 95% Prediction Intervals (Eqs. (4) and (5)).
- Step 4: Hh was estimated, in function of every D in the range, with the central hub height MHhD model (Eq. (7)), as well as with the 95% Prediction Intervals (Eqs. (8) and (9)).
- Step 5: $k2$ and $c2$ were calculated, for every Hh from Step 4, with the JM model (Eqs. (17), (20) and (21)).
- Step 6: With $Rn = 1{,}000$ Riemann rectangles, E was calculated with Eqs. (22)–(29) for every D and with seven different ways of calculating $\hat{\eta}$ and $\hat{Hh}$. This resulted in the seven curves shown in Fig. 23(a) which delimit the uncertainty related to different assumptions. The central estimates (central continuous line) were established by assuming $\hat{\eta} = MED$ and $\hat{Hh} = MHhD$. The outermost interval ranges from a curve calculated using $\hat{\eta} = \eta_{95high}$ and $\hat{Hh} = Hh_{95high}$ to a curve with $\hat{\eta} = \eta_{95low}$ and $\hat{Hh} = Hh_{95low}$. The "MED 95%PI" interval ranges from a curve with $\hat{\eta} = \eta_{95high}$ and $\hat{Hh} = MHhD$ to a curve with $\hat{\eta} = \eta_{95low}$ and $\hat{Hh} = MHhD$. Lastly, the "MHhD 95%PI" interval ranges from a curve with $\hat{\eta} = MED$ and $\hat{Hh} = Hh_{95high}$ to a curve with $\hat{\eta} = MED$ and $\hat{Hh} = Hh_{95low}$.

The intervals in Fig. 23(a) serve as a practical illustration of the effect over $\hat{E}$ due to the expected uncertainty related to the MED model alone, the MHhD model alone, and the combined effect of both 95% Prediction Intervals. The wider the interval, the more influence it can have in terms of $\hat{E}$ uncertainty. At first sight, the uncertainty related to MED alone appears to be more influential than the one of MHhD. However, as it can be seen in the Close-up, MHhD surpasses the influence of the MED uncertainty for smaller diameters. This can also be perceived in Fig. 23(b), where the heights of the intervals at every point are plotted as proportions of the estimates of the central curve. Here, it was found that the uncertainty of MHhD becomes more influential below $D = 41.37$ m (within the broad assumptions of this analysis).

6.4. Estimation of the Cost of Energy

Step 7 consists in the calculations needed, for every potential wind turbine, to estimate the total *Cost of Energy* (C_E) in [USD/Wh]. First, it must be defined what proportion of the capital cost for the whole wind project is represented by the wind turbines (WT_p). A reference value $WT_p = 0.69$ [40] may be used for generic or preliminary estimations. Then, it is established the proportion of the operating and maintenance costs in terms of the capital cost for the whole wind project (m). If the costs related to land use are not included, a reasonable assumption may be $m = 1.5$–2% [40,39]. 3.5% may be used instead if land rent is also considered [40]. Lastly, the *Real Rate of Interest* (I) must be defined for the financing of the project. $I = 0.05$ may be assumed for generic estimations [40]. C_E can then be calculated with Eq. (30).

$$C_E = \frac{C_{wt}}{WT_p E}\left[1 + m\left(\frac{(1+I)^{Life}-1}{I(1+I)^{Life}}\right)\right] \tag{30}$$

What this equation does is to calculate the total costs associated with the wind project throughout the expected lifespan and divide it by the total energy that is expected to be generated. The result, in [USD/W h], allows making comparisons with the local energy market. If the cost of energy in the local market is higher than C_E, then this implies that using the wind project to directly consume the energy output may be worth it, and money could be saved that would have been used otherwise for buying energy from the public grid. Furthermore, if the state buys renewable energy at a higher rate than C_E, then this implies that a profit could be made if the purpose of the project is to sell energy.

Continuing the analysis presented in Fig. 23(a), Fig. 24(a) shows a generic analysis of how C_E may behave for a range of rotor diameters. For this analysis, the same steps described at the end of Section 6.3 were taken up to Step 7 of the proposed method (Fig. 20). C_{wt} was generically calculated in function of P_R with Eq. (15) and C_E was obtained with Eq. (30).

As the expression used to calculate C_{wt} presents three broad rates for different P_R ranges, the main central curve in Fig. 24(a) evidences a stepped-like behavior. The effects of the 95% Prediction Intervals were calculated only around this central stepped curve (the central continuous line). However, the close-up in the figure also shows, with the

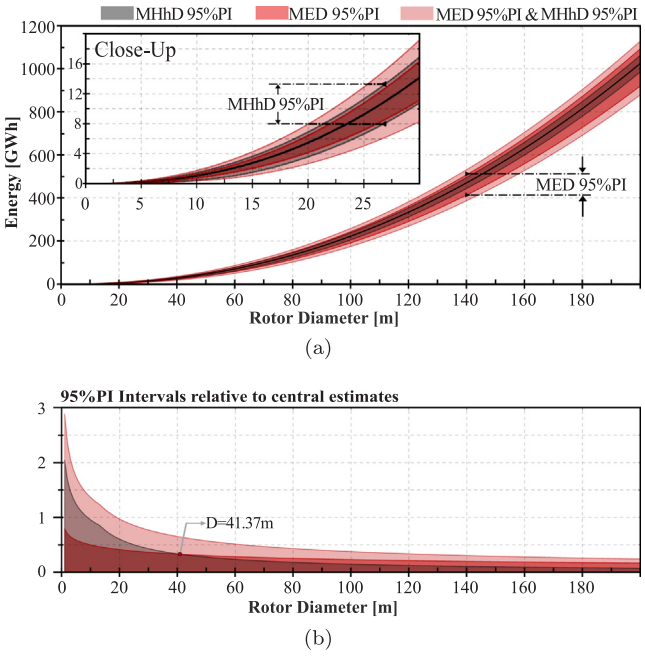

Fig. 23. Energy output in function of D considering the uncertainty through different 95% Prediction Intervals, defined in (a) for both subfigures.

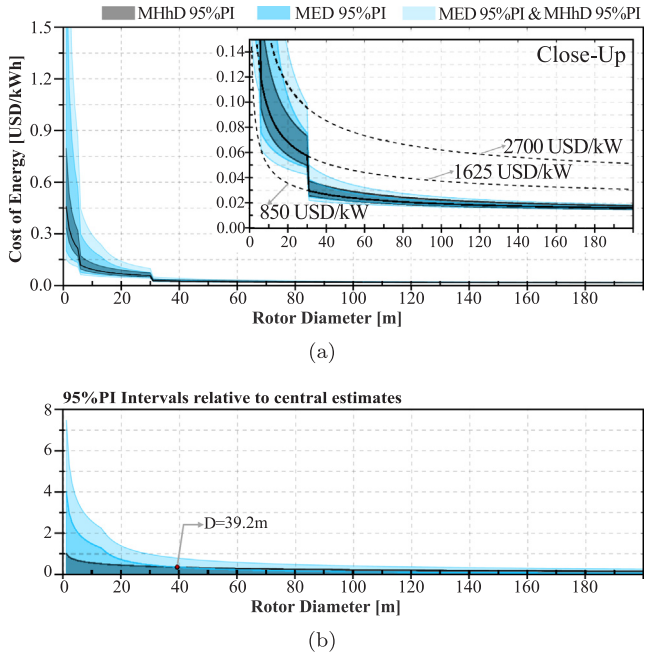

Fig. 24. Cost of energy in function of D considering the uncertainty through different 95% Prediction Intervals, defined in (a) for both subfigures.

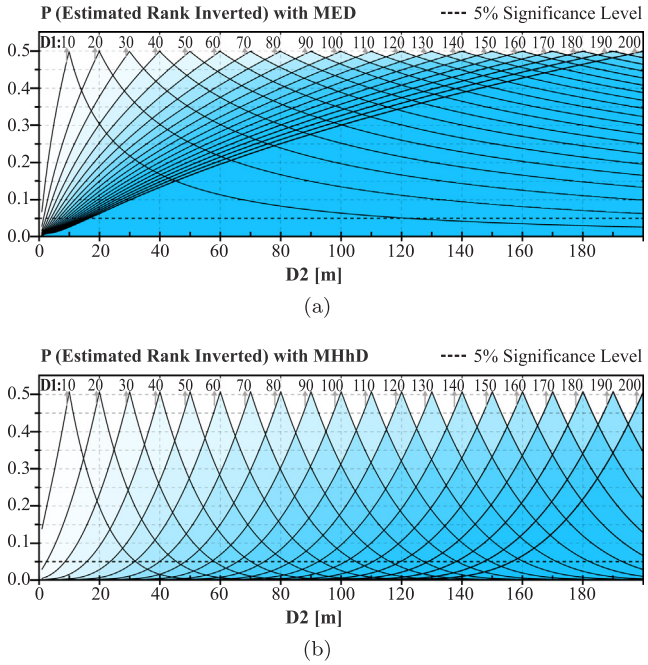

Fig. 25. Stochastic rank dominance analyzes for pairs of turbines in terms of (a) $\hat{\eta}$ and (b) $\widehat{Hh}$.

dashed curves, the behavior of the central estimates (i.e., with $\hat{\eta} = MED$ and $\widehat{Hh} = MHhD$) when each cost rate is projected throughout the entire D range. This illustrates the critical impact of estimating C_{wt} from different assumptions.

Fig. 24(b) shows the heights of the intervals at every point plotted as proportions of the central estimates. Here, it was found that MHhD becomes more influential below $D = 39.2$ m in terms of how its uncertainty may affect $\widehat{C_E}$. This makes intuitive sense for the following reasons. The wind gains due to the extrapolation of the Weibull parameters present diminishing returns as height becomes larger. The 95% PI uncertainty of the MHhD model has a greater impact on the energy that can be generated by smaller turbines because, as they tend to be closer to the ground, the effect of varying Hh causes larger gains or losses in the average wind strength. This effect reduces proportionally as D increases. On the other hand, the 95% PI uncertainty of the MED model evidences a proportional impact that is less influenced by D and which is similar in magnitude for both E and C_E.

6.5. Preliminary selection

Steps 8–10 go from selecting the fittest WTs to assessing the estimated rank uncertainty and enabling a preliminary decision. In Step 8, the best two wind turbines are selected on the basis of the C_E estimations. The C_E values of these two turbines imply an estimated rank that establishes which one is tentatively the best option. Steps 9 and 10 assess the probability that the estimated ranks in $\hat{\eta}$ (Eq. (6)) and $\widehat{Hh}$ (Eq. (10)) are the inverse of the actual ranks. The lower the probability, the more one can rely on the estimated ranks.

The user of the proposed method must then decide whether the resulting level of uncertainty is acceptable. If it is not enough for a preliminary selection, then more information and further analyzes are needed, such as trying to find trustworthy Power Curves for the WTs considered. This would allow to calculate η without the uncertainty related to MED.

$P_{\Delta\hat{\eta}invert}$ and $P_{\Delta\widehat{Hh}invert}$ are in function of the difference in $\hat{\eta}$ and $\widehat{Hh}$ between pairs of turbines. However, as both $\hat{\eta}$ and $\widehat{Hh}$ were established in function of D, it is of interest to analyze how $P_{\Delta\hat{\eta}invert}$ and $P_{\Delta\widehat{Hh}invert}$ behave with the difference between two given rotor diameters $D1$ and $D2$. Addressing this in terms of $P_{\Delta\hat{\eta}invert}$, Fig. 25(a) presents 20 curves corresponding to 20 different $D1$ values. Each curve is plotted throughout a range of possible paired $D2$ values. At every point of every curve, $\hat{\eta}$ is estimated for both $D1$ and $D2$ and the absolute difference between them is used to estimate $\widehat{P_{\Delta\hat{\eta}invert}}$ (shown in the Y-axis).

These curves can serve as an intuitive guide to understand how different must a $D2$ be from a given $D1$ in order to reach a 5% significance level. For instance, if $D1 = 10$ m, $\widehat{P_{\Delta\hat{\eta}invert}}$ is 6.8% when $D2 = 1$ m and the significance line is crossed when $D2 \geq 122.04$ m. Thus, a −9 m difference in D achieves a result similar to a + 112.04 m difference. This is because, as MED involves a large transformation of D (similar to a logarithmic transformation), a greater change in $\hat{\eta}$ is expected for smaller diameters. This, in turn, implies a greater impact in terms of $\widehat{P_{\Delta\hat{\eta}invert}}$. This is also the reason why the larger $D1$ is, the larger the difference with $D2$ needed to reach a given significance level. In this analysis, it can be evidenced that an increment in D presents diminishing returns regarding $\hat{\eta}$ improvements.

Fig. 25(b) presents the same analysis but in terms of $\widehat{Hh}$. Here, contrary to the previous results, the 20 curves corresponding to the different $D1$ values have similar shapes. This is because the relation between $\widehat{Hh}$ and D (untransformed) is almost linear, and the transformation required ($\lambda = 0.69$) has a modest effect compared to the one used in MED ($\lambda = 0.01$). Therefore, any given difference $D1-D2$ implies a similar difference in $\widehat{Hh}$ and $\widehat{P_{\Delta\widehat{Hh}invert}}$. For instance, with $D1 = 40$ m, a result of 5% is reached when $D2 = 15.75$ m or $D2 = 70.2$ m. In this case, the difference in D needed for a 5% significance is around 24–30 m. A similar trend was found for other $D1$ curves, but with an increasing difference required as $D1$ increases. This can be evidenced in Fig. 25(b), where the curves become slightly wider from left to right.

7. Conclusions

With the increasing democratization and adoption of wind energy, more and more non-experts are being urged to choose among a broad range of commercial offers. In this regard, the cost of energy is a comprehensive and objective performance indicator that can provide a valuable orientation. However, reportedly misleading publicity and commonly unavailable information make this selection process more

inaccessible and unreliable. For instance, an evident mismatch was found between the power curve of the XZERES 442 provided by ARE and the one characterized by the third-party NREL. In another instance, it was found that the rated power and rated wind speed of the CF20 was not in agreement with a certification power curve developed by Intertek. This work addresses this situation with a new method for comparing wind turbines based on nominal specifications. The misleading or unavailable information gap was overcome by estimating key needed variables (the total efficiency and a tentatively feasible hub height) through the statistical analysis of trends in a dataset of 176 WTs.

A clear trend was found between the rated power and the rotor diameter. A fitted regression model, of the form $Y = \alpha X^{\beta}$, was in agreement with previously reported models. The estimations with this model were found to imply a deviation in magnitude of 547.7 kW on average.

The relation between the total efficiency, as the response variable, in function of the rotor diameter, as predictor, was effectively linearized with the Tukey's Ladder of powers. Through a 5-fold cross-validation procedure, the best fitting performance was found with the predictor raised to the power of 0.01. The selected model, established as MED (Model of Efficiency in function of Diameter), resulted in $\bar{r} = 0.78$, $\overline{R^2} = 0.608$, and $\overline{RMSE} = 0.0462$ in the training set. In an evaluation with the testing set, MED achieved $r = 0.758$, $R^2 = 0.574$, and $RMSE = 0.0562$. With Monte Carlo randomization analyzes, it was found that the linear response (Slope) in MED was highly significant and no systematic trends were found in its residuals.

Similarly, the relation between the hub height and the diameter, as predictor, was effectively linearized by transforming the diameter raised to the power of 0.69. This model, established as MHhD (Model of Hub height in function of Diameter), resulted in $\bar{r} = 0.96$, $\overline{R^2} = 0.921$, and $\overline{RMSE} = 10.0441$ in the training set, and $r = 0.974$, $R^2 = 0.948$, and $RMSE = 8.9011$ in the testing set. No systematic trends were found in its residuals and its Slope resulted highly significant. This suggests that the linear response is highly unlikely to be explained by randomness alone and, thus, the trend characterized by MHhD is assumed as real.

From the analysis of the MED Prediction Intervals, it was calculated that new efficiency values are expected to fall 95% of the times within + 0.101 and −0.114 around the central estimates. 11.1% of the testing data were outside this range, but the difference between their magnitude and the limits of the range was, on average, just 2.53%. In the case of MHhD, the 95% interval goes, on average, from + 22.22 m to − 19.63 m around the central hub height estimates. 6.3% of the testing data were outside this range, with 0.44% difference between their magnitude and the limits of the prediction interval. This suggests that the prediction intervals of both models provide a reasonable estimation of the range where the efficiency and hub height of most turbines would probably fall.

It was observed that the uncertainty regarding the 95% Prediction Interval of MHhD, in terms of energy and cost of energy, had a steeper response in function of the diameter compared to the effect of MED's uncertainty. Also, MHhD's uncertainty was found to become more influential below a diameter of 41.37 m, for energy calculations, and 39.2 m, for cost of energy calculations. Therefore, for smaller turbines, the accuracy in the hub height estimation is more critical than the efficiency estimation.

It was calculated that a difference in efficiency between two turbines of at least 0.1069 is needed to reach a 5% significance level in terms of stochastic rank dominance. In other words, beyond this threshold, it is unlikely that an efficiency rank between two given turbines, estimated with MED, is the opposite of the actual rank. In the case of comparing two turbines in terms of their hub height, the difference must be of at least 23.35 m for a 5% significance level. Moreover, it was found that the larger a rotor is, the more difference in diameter is needed compared to another turbine to achieve a significant stochastic rank dominance in terms of efficiency and hub height. However, even in the cases where the estimated ranks are not significant, they may provide a valuable guide for a preliminary selection, or to narrow down the choices, whenever limited information frustrates more detailed performance analyzes.

The models proposed and validated in this work are based on a dataset that represents only a subset of the total population of commercialized Horizontal Axis Wind Turbines. Thus, the parameters of these models might be influenced by the possible biases in the dataset. In further work, the validity of the proposed models can be further tested with other datasets and by considering other possible combinations of predictor variables. Also, the applicability of the selection method can be evaluated in case studies.

Acknowledgements

Special thanks to Universidad EAFIT through the postgraduate studies grant "Undergraduate research excellence scholarship". Also, special thanks to Colciencias (Colombian Administrative Department of Science, Technology and Innovation) and, again, Universidad EAFIT, who jointly sponsored the "Young Researchers and Innovators Program" in the 645-2014 and 761-2016 calls. This research has also been developed in the framework of the Research Program "ENERGETICA 2030", code 58667, funded by the World Bank through Colciencias' 778-2017 call - Scientific Ecosystem.

Appendix A. Supplementary material

Supplementary data associated with this article can be found, in the online version, at http://dx.doi.org/10.1016/j.apenergy.2018.06.103.

References

[1] Cook J, Nuccitelli D, Skuce A, Jacobs P, Painting R, Honeycutt R, et al. Reply to quantifying the consensus on anthropogenic global warming in the scientific literature: a re-analysis. Energy Policy 2014;73:706–8.
[2] Cherian J, Jacob J. Green marketing: a study of consumers attitude towards environment friendly products. Asían Social Sci 2012;8(12):117.
[3] Cheng M, Zhu Y. The state of the art of wind energy conversion systems and technologies: a review. Energy Convers Manage 2014;88:332–47.
[4] Bukala J, Damaziak K, Kroszczynski K, Krzeszowiec M, Malachowski J. Investigation of parameters influencing the efficiency of small wind turbines. J Wind Eng Ind Aerodyn 2015;146:29–38.
[5] Dai K, Bergot A, Liang C, Xiang W-N, Huang Z. Environmental issues associated with wind energy—a review. Renew Energy 2015;75:911–21.
[6] Bhutta MMA, Hayat N, Farooq AU, Ali Z, Jamil SR, Hussain Z. Vertical axis wind turbine—a review of various configurations and design techniques. Renew Sustain Energy Rev 2012;16(4):1926–39.
[7] Bai C, Hsiao F, Li M, Huang G, Chen Y. Design of 10 kW horizontal-axis wind turbine (hawt) blade and aerodynamic investigation using numerical simulation. Procedia Eng 2013;67:279–87.
[8] Arbeloa Sola L. Dise no de un aerogenerador de eje vertical tipo savonius para electrificación rural, PFC. Acceso abierto. < https://academica-e.unavarra.es/handle/2454/6667 > .
[9] Perkin S, Garrett D, Jensson P. Optimal wind turbine selection methodology: a case-study for Búrfell, Iceland. Renew Energy 2015;75:165–72.
[10] Gipe P. Wind energy basics: a guide to home and community-scale wind-energy systems. Chelsea Green Publishing; 2009.
[11] Danny Harvey L. Energy and the new reality 2 carbon-free energy supply. Biomass energy. Routledge, Earthscan LLC 1616; 2010. p. 173–279.
[12] McTavish S, Feszty D, Nitzsche F. Evaluating Reynolds number effects in small-scale wind turbine experiments. J Wind Eng Ind Aerodyn 2013;120:81–90.
[13] Kishore RA, Coudron T, Priya S. Small-scale wind energy portable turbine (swept). J Wind Eng Ind Aerodyn 2013;116:21–31.
[14] Bak C. Sensitivity of key parameters in aerodynamic wind turbine rotor design on power and energy performance. J Phys: Conf Ser 2007;75(1):012008 < http://stacks.iop.org/1742-6596/75/i=1/a=012008 > .
[15] Hren S, Hren R. A solar buyer's guide for the home and office: Navigating the maze of solar options, incentives, and installers. Chelsea Green Publishing; 2010. ISBN: 1603583084.
[16] Caduff M, Huijbregts MA, Althaus H-J, Koehler A, Hellweg S. Wind power electricity: the bigger the turbine, the greener the electricity? Environ Sci Technol 2012;46(9):4725–33.
[17] Ederer N. The right size matters: investigating the offshore wind turbine market equilibrium. Energy 2014;68:910–21.
[18] Sieros G, Chaviaropoulos P, Sørensen JD, Bulder B, Jamieson P. Upscaling wind turbines: theoretical and practical aspects and their impact on the cost of energy.

Wind Energy 2012;15(1):3–17.
[19] Alam MM, Rehman S, Meyer JP, Al-Hadhrami LM. Review of 600–2500 kW sized wind turbines and optimization of hub height for maximum wind energy yield realization. Renew Sustain Energy Rev 2011;15(8):3839–49.
[20] Chen K, Song M, Zhang X. The iteration method for tower height matching in wind farm design. J Wind Eng Ind Aerodyn 2014;132:37–48.
[21] Mirhosseini M, Sharifi F, Sedaghat A. Assessing the wind energy potential locations in province of Semnan in Iran. Renew Sustain Energy Rev 2011;15(1):449–59.
[22] Hadi FA. Diagnosis of the best method for wind speed extrapolation. Int J Adv Res Electr, Electron Instrum Eng 2015;4(10).
[23] Gualtieri G, Secci S. Methods to extrapolate wind resource to the turbine hub height based on power law: a 1-h wind speed vs. Weibull distribution extrapolation comparison. Renew Energy 2012;43:183–200.
[24] Bezrukovs VP, Bezrukovs VV, Zacepins AJ. Comparative efficiency of wind turbines with different heights of rotor hubs: performance evaluation for latvia. J Phys: Conf Ser 2014;524(1):012113 <http://stacks.iop.org/1742-6596/524/i=1/a=012113>.
[25] Mikhail A. Height extrapolation of wind data. J Solar Energy Eng 1985;107(1):10–4.
[26] Lassig J, Colman J. Wind turbines aerodynamics. Applied aerodynamics. InTech; 2012.
[27] Montoya FG, Manzano-Agugliaro F, López-Márquez S, Hernández-Escobedo Q, Gil C. Wind turbine selection for wind farm layout using multi-objective evolutionary algorithms. Expert Syst Appl 2014;41(15):6585–95.
[28] Drew D, Barlow J, Cockerill T. Estimating the potential yield of small wind turbines in urban areas: a case study for greater London, UK. J Wind Eng Ind Aerodyn 2013;115:104–11.
[29] Shaw S, Rosen A, Beavers D, Korn D, Fund MRET, et al. Status report on small wind energy projects supported by the Massachusetts Renewable Energy Trust. Massachusetts Renew Energy Trust Fund 2008.
[30] Üstüntaş T, Şahin AD. Wind turbine power curve estimation based on cluster center fuzzy logic modeling. J Wind Eng Ind Aerodyn 2008;96(5):611–20.
[31] Li S, Wunsch DC, O'Hair E, Giesselmann MG. Comparative analysis of regression and artificial neural network models for wind turbine power curve estimation. J Sol Energy Eng 2001;123(4):327–32.
[32] Janssens O, Noppe N, Devriendt C, Van de Walle R, Van Hoecke S. Data-driven multivariate power curve modeling of offshore wind turbines. Eng Appl Artif Intell 2016;55:331–8.
[33] Díaz S, Carta JA, Matías JM. Performance assessment of five mcp models proposed for the estimation of long-term wind turbine power outputs at a target site using three machine learning techniques. Appl Energy 2018;209:455–77.
[34] Coma E, Jones P. buildings as power stations: an energy simulation tool for housing. Procedia Eng 2015;118:58–71.
[35] RWE npower renewables. Wind turbine power calculations. Mechanical and electrical engineering power industry. The Royal Academy of Engineering; 2012.
[36] El-Shimy M. Optimal site matching of wind turbine generator: case study of the gulf of suez region in Egypt. Renew Energy 2010;35(8):1870–8.
[37] Jowder FA. Wind power analysis and site matching of wind turbine generators in Kingdom of Bahrain. Appl Energy 2009;86(4):538–45.
[38] Arias-Rosales A, Osorio-Gómez G. Data-set with the nominal specifications and efficiency estimations of hawt wind turbines. http://dx.doi.org/10.17632/2h6k9sfb7k.1.
[39] Fazelpour F, Soltani N, Soltani S, Rosen MA. Assessment of wind energy potential and economics in the north-western iranian cities of Tabriz and Ardabil. Renew Sustain Energy Rev 2015;45:87–99.
[40] Mathew S. Economics of wind energy. Berlin, Heidelberg: Springer Berlin Heidelberg; 2006. p. 209–36. http://dx.doi.org/10.1007/3-540-30906-3_7.
[41] Sedaghat A, Hassanzadeh A, Jamali J, Mostafaeipour A, Chen W-H. Determination of rated wind speed for maximum annual energy production of variable speed wind turbines. Appl Energy 2017;205(Suppl. C):781–9. http://dx.doi.org/10.1016/j.apenergy.2017.08.079 <http://www.sciencedirect.com/science/article/pii/S0306261917310978>.
[42] Vasel-Be-Hagh A, Archer CL. Wind farm hub height optimization. Appl Energy 2017;195(Suppl. C):905–21. http://dx.doi.org/10.1016/j.apenergy.2017.03.089 <http://www.sciencedirect.com/science/article/pii/S0306261917303306>.
[43] Bowen A, Huskey A, Link H, Sinclair K, Forsyth T, Jager D, et al. Small wind turbine testing results from the national renewable energy lab. Tech rep. Golden, CO: National Renewable Energy Laboratory (NREL); 2009.
[44] Intertek Testing Services NA, Inc. Wind certification program directory. < www.intertek.com/wind/directory/ > .
[45] Fields J, Oteri F, Preus R, Baring-Gould I. Deployment of wind turbines in the built environment: risks, lessons, and recommended practices. Tech rep. NREL (National Renewable Energy Laboratory (NREL), Golden, CO (United States)); 2016.
[46] SMALL WIND CERTIFICATION COUNCIL. Information for consumers: certified wind turbine models and consumer labels; 2017. < http://smallwindcertification.org/for-consumer/ > .
[47] Allan G. En-4153-a: Orenda skye mcs summary report. Version a. Tech rep. Orenda Energy Solutions Inc.; 2017 <http://orendaenergy.com/wp-content/uploads/2017/05/EN-4153-A-Orenda-Skye-MCS-Summary-Report.pdf>.
[48] GL Garrad Hassan's WINDTEST. Mcs certification summary for tn535 swt. Tech rep. GL Garrad Hassan's WINDTEST; 2015 <http://www.tozzigreen.com/contrib/uploads/TN-12-057_MCS_Summary_TN535_rev2-3.pdf>.
[49] Eocycle. Eocycle obtains prototype certification for eocycle 25 in denmark; 2014. < http://eocycle.com/ > .
[50] Smith J, Huskey A, Jager D, Hur J. Wind turbine generator system power performance test report for the entegrity ew50 wind turbine. Contract 2011;303:275–3000.
[51] Mendoza I, Hur J, Thao S, Curtis A. Power performance test report for the us department of energy 1.5-megawatt wind turbine. Tech rep. Golden, CO (United States): National Renewable Energy Laboratory (NREL); 2015.
[52] Mendoza I, Hur J. Power performance test report for the swift wind turbine. Tech rep. Golden, CO: National Renewable Energy Laboratory (NREL); 2012.
[53] Gipe P. Wind power: renewable energy for home, farm, and business. 2nd ed. Chelsea Green Publishing; 2004.
[54] Hailes D. Warwick wind trials project (wwtp) final report. Tech rep. Encraft; 2009 <www.microwindturbine.be/Welkom.html>.
[55] Summerville B. Small wind turbine performance in western North Carolina. Appalachian State University; 2005.
[56] Mertens S. Resultaten testveld kleine windturbines schoondijke, rapport 1001214.r03. Tech rep. Ingreenious BV; 2012 <www.zeeland.nl/digitaalarchief/zee1300980>.
[57] Vick BD, Clark RN, Drawer P. Performance and acoustic analysis of a small wind turbine used with a helical pump for livestock watering. Proceedings of AWEA windpower 2005 conference. 2005.
[58] Sustainable Technologies Evaluation Program (STEP). Technical assessment of small wind turbine power generation. Technical brief. Tech rep. Toronto and Region Conservation Authoritys Sustainable Technologies Evaluation Program (STEP); 2015. < http://www.sustainabletechnologies.ca/wp/wp-content/uploads/2015/09/WindTurb_TechBrief_Sept2015.pdf > .
[59] Engels W, Obdam T, Savenije F. Current developments in wind – 2009: going to great lengths to improve wind energy. Tech rep. Energy research Centre of the Netherlands (ECN); 2009.
[60] Newville M, Stensitzki T, Allen D, Ingargiola A. Non-linear least-squares minimization and curve-fitting for python. Chicago, IL; 2015.
[61] Wistuba M, Schilling N, Schmidt-Thieme L. Hyperparameter search space pruning – a new component for sequential model-based hyperparameter optimization. In: Appice A, Rodrigues PP, Santos Costa V, Gama J, Jorge A, Soares C, editors. Machine learning and knowledge discovery in databases. Cham: Springer International Publishing; 2015. p. 104–19.
[62] Pruim R, Kaplan DT, Horton NJ. The mosaic package: helping students to 'think with data' using r. R J 2017;9(1):77–102 <https://journal.r-project.org/archive/2017/RJ-2017-024/index.html>.
[63] Faraway JJ. Linear models with R. CRC Press; 2014.
[64] Tukey JW. Exploratory data analysis, vol. 2. Reading, Mass.; 1977.
[65] Duan N. Smearing estimate: a nonparametric retransformation method. J Am Stat Assoc 1983;78(383):605–10.
[66] Welch GW. Model fit and interpretation of non-linear latent growth curve models [Ph.D. Thesis]. University of Pittsburgh; 2007.
[67] Mudelsee M. Correlation. Netherlands, Dordrecht: Springer; 2010. p. 285–338. http://dx.doi.org/10.1007/978-90-481-9482-7_7.
[68] Cleff T. Regression analysis. Cham: Springer International Publishing; 2014. p. 115–45. http://dx.doi.org/10.1007/978-3-319-01517-0_5.
[69] Gotelli N, Ellison A. A primer of ecological statistics. Macmillan Education; 2013 <https://books.google.com.co/books?id=zTbjMQEACAAJ>.
[70] Manly BF. Randomization. Bootstrap and Monte Carlo methods in biology vol. 70. CRC Press; 2006.
[71] Ewens WJ. On estimating p values by monte carlo methods. Am J Human Genet 2003;72(2):496.
[72] Lins ID, Droguett EL, das Chagas Moura M, Zio E, Jacinto CM. Computing confidence and prediction intervals of industrial equipment degradation by bootstrapped support vector regression. Reliab Eng Syst Saf 2015;137:120–8.
[73] Dinno A. Nonparametric pairwise multiple comparisons in independent groups using dunns test. Stata J 2015;15:292–300.
[74] Spera D, Richards T. Modified power law equations for vertical wind profiles. Wind Charact Wind Energy Siting Conf 1979.
[75] Cavcar M. The international standard atmosphere (isa) vol. 30. Turkey: Anadolu University; 2000. p. 9.
[76] Seguro J, Lambert T. Modern estimation of the parameters of the weibull wind speed distribution for wind energy analysis. J Wind Eng Ind Aerodyn 2000;85(1):75–84.
[77] SITES DRM. Evaluation of the adequacy of the wind speed extrapolation laws for two different roughness meteorological sites. Am J Appl Sci 2014;11(4):570–83.
[78] Manwell JF, McGowan JG, Rogers AL. Wind energy explained: theory, design and application. John Wiley & Sons; 2010.
[79] Peacock A, Jenkins D, Ahadzi M, Berry A, Turan S. Micro wind turbines in the uk domestic sector. Energy Build 2008;40(7):1324–33.
[80] Oyedepo SO, Adaramola MS, Paul SS. Analysis of wind speed data and wind energy potential in three selected locations in south-east nigeria. Int J Energy Environ Eng 2012;3(1):7.
[81] Davis PJ, Rabinowitz P. Methods of numerical integration. Courier Corporation; 2007.